

# Long-term photometric observations of pre-main sequence objects in the field of North America/Pelican Nebula<sup>★</sup>

I. Poljančić Beljan<sup>1</sup>, R. Jurdana-Šepić<sup>1</sup>, E. H. Semkov<sup>2</sup>, S. Ibryamov<sup>2</sup>, S. P. Peneva<sup>2</sup>, and M. K. Tsvetkov<sup>2</sup>

<sup>1</sup> Physics Department, University of Rijeka, Radmile Matejčić 2, 51000 Rijeka, Croatia  
e-mail: jurdana@phy.uniri.hr

<sup>2</sup> Institute of Astronomy and National Astronomical Observatory, Bulgarian Academy of Sciences, 1784 Sofia, Bulgaria

Received 1 November 2013 / Accepted 16 June 2014

## ABSTRACT

To broaden the search and study stars in the early evolutionary phase, we investigated a sample of 17 pre-main sequence objects previously detected as either  $H\alpha$  emission-line pre-main sequence stars or T Tauri variables located in the field of the North America/Pelican Nebula complex. Johnson-Cousins  $B$ ,  $V$ ,  $R_c$ ,  $I_c$  magnitudes and mean color indices for the program stars are determined from more than 12 400 measurements from archive photographic plates and from CCD data collected at 7 observatories covering the period of almost 60 years from 1954 up to 2013. We complemented previously rare insights on the photometry of the program stars and presented their photometric history, which for almost all program stars is the first long term photometric monitoring on a timescale of 6 decades. Eight program stars are found to be classical T Tauri stars of variability type II, while 6 program stars are weak-line T Tauri stars of variability type I. For the first time, periodicity is found for three stars: V1716 Cyg indicates a 4.15 day period, V2051 Cyg indicates a 384 day period, and V521 Cyg a period of 503 days.

**Key words.** stars: pre-main sequence – stars: variables: general

## 1. Introduction

Long term variability surveys of pre-main sequence (PMS) stars, both photometric and spectroscopic, are very important for understanding the early stages of stellar evolution. They target active star forming regions with the aim of discovering and quantifying their variability in terms of amplitude, timescale, and recurrence. PMS stars are comparatively rare among field stars because the evolutionary phase they are undergoing is short, since contraction toward the main sequence takes up less than 1% of a star's life. Adding to this, observations of PMS stars are usually made difficult by their faintness in quiescence and by the disturbance from sometimes heavy dust extinction, either surrounding the star or diffuse through the star forming region. Therefore, the rare outbursts of PMS stars always attract considerable interest, especially when they are long lasting, as in the case of new FUor objects (from the name of the prototype of this class, FU Ori), with one of the most recent and spectacular cases being that of HBC 722 = V2493 Cyg (Semkov et al. 2010; Miller et al. 2011; Munari et al. 2010; Leoni et al. 2010; Kóspál et al. 2011; Armond et al. 2011; Green et al. 2011).

One of the most frequent types of PMS stars are the T Tauri stars (TTS) – young, low-mass stars ( $M \leq 2 M_{\odot}$ ) still contracting towards the main sequence (Joy 1942, 1945). Some exhibit strong brightness variations over comparatively short time intervals (days, months) with brightness increases of up to several magnitudes in some photometric bands. Ménard & Bertout (1999) reviewed their properties and divided them into two subgroups; classical T Tauri stars (CTTS) still actively accreting from their circumstellar disks and the weak-line T Tauri stars (WTTS) without evidence of disk accretion. Herbst et al. (1994)

described three types of day to week timescale variability of TTS: type I variability, most often seen in WTTSs characterized by (i) a low level periodic modulation of the stellar flux and results from the rotation of a cool spotted photosphere; (ii) type II variations with larger photometric amplitudes (up to 2 or 3 mag) that are often irregular but sometimes periodic and associated with short-lived accretion-related events on the stellar surface of CTTS; and (iii) more rarely observed type III variations, characterized by luminosity dips lasting from a few days up to several months, which presumably result from circumstellar dust obscuration and are associated with the so-called UXors.

The photometric and spectroscopic parameters of CTTS are modulated by rotation due to surface temperature inhomogeneities induced by magnetic activity and mass accretion. Artemenko et al. (2012) have recently derived the periods and amplitudes of the rotational modulation of brightness and color for 31 CTTS. One of the first opportunities to investigate the long-term variability of a significant sample of CTTS was 20 year long photometric database provided by Grankin et al. (2007, 2008).

One of the most notable and well studied areas of star formation in the northern sky is the region of the North America/Pelican Nebula complex. Since Herbig's (1958) discovery, it has been known to contain a number of PMS stars, among which are T Tauri and  $H\alpha$  emission stars, Herbig-Haro objects, and flare stars from the UV Ceti type (Armond et al. 2011; Semkov et al. 2012; Findeisen et al. 2013). The largest number of young stars are found in the so-called Pelican Nebula (IC 5070), a few in the North America (NGC 7000) near "Florida", and in the "Gulf of Mexico" region between the two nebulas (Corbally et al. 2009).

To broaden the search and investigations of stars in the PMS evolutionary phase, we undertook a long-term photometric study for the sample of 17 stars in the field of North America/Pelican

<sup>★</sup> Full Tables 4 and 5 are only available at the CDS via anonymous ftp to [cdsarc.u-strasbg.fr](http://cdsarc.u-strasbg.fr) (130.79.128.5) or via <http://cdsarc.u-strasbg.fr/viz-bin/qcat?J/A+A/568/A49>

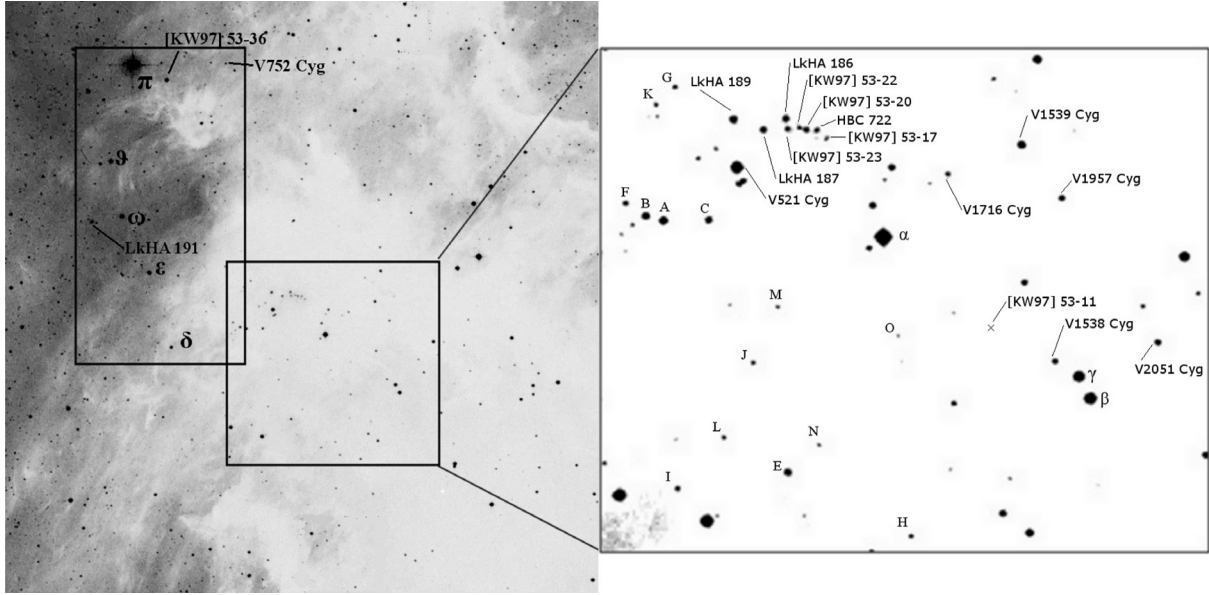


**Fig. 1.** Finding chart for the sample stars and the used *BVRI* comparison sequence around V2493 Cyg (A to O and  $\alpha\beta\gamma\delta\epsilon\omega\theta\pi$ ).

**Table 1.** List and coordinates of program stars.

GCVS <sup>1</sup>	[KW 97] <sup>2</sup>	HBC <sup>3</sup>	LkH $\alpha$ <sup>4</sup>	$\alpha$ (J2000.0)	$\delta$ (J2000.0)
	<b>53-11</b>			20 58 03.0	+43 50 42
	<b>53-17</b>			20 58 16.261	+43 53 34.94
	<b>53-36</b>			20 58.8	+44 03
	<b>53-20</b>			20 58 17.906	+43 53 44.13
	<b>53-22</b>			20 58 18.503	+43 53 46.02
	<b>53-23</b>			20 58 19.515	+43 53 45.00
	53-24	723	<b>186</b>	20 58 19.615	+43 53 54.52
	53-25	724	<b>187</b>	20 58 21.543	+43 53 44.96
	53-27	725	<b>189</b>	20 58 24.008	+43 53 54.61
	53-42	301	<b>191</b>	20 59 05.82	+43 57 03.1
<b>V521 Cyg</b>	53-26	299	188	20 58 23.811	+43 53 11.45
<b>V752 Cyg</b>	53-30			20 58 33.6	+44 03 32
<b>V1538 Cyg</b>				20 57 57.505	+43 50 08.95
<b>V1539 Cyg</b>	53-9	720	185	20 57 59.864	+43 53 26.00
<b>V1716 Cyg</b>				20 58 06.116	+43 53 01.17
<b>V1957 Cyg</b>				20 57 56.52	+43 52 36.3
<b>V2051 Cyg</b>				20 57 48.804	+43 50 23.60

**Notes.** Star identifiers used in this paper are marked in boldface.

**References.** <sup>(1)</sup> General Catalogue of Variable Stars; <sup>(2)</sup> Kohoutek & Wehmeyer (1997); <sup>(3)</sup> Herbig & Bell (1988); <sup>(4)</sup> Herbig (1958).

Nebula complex. The target stars were selected among those listed in SIMBAD as either H $\alpha$  emission line stars, PMS stars, or T Tau variables. Photometric information, especially concerning long-term behavior, is missing in literature for all of them except for LkH $\alpha$  191, V521 Cyg, V1539 Cyg, and V1716 (Grankin et al. 2007; Findeisen et al. 2013; Artemenko et al. 2012).

## 2. Star sample and measurements

We carried out a CCD *BVRI* photometric observational program for 17 stars (listed in Table 1 with the finding chart in Fig. 1) in the field of V2493 Cyg (“Gulf of Mexico”). The star sample was extracted from the SIMBAD astronomical database by exact object types (Or – variable star of Orion type, Fl – flare star, Em – emission line star) and with the condition on their location – positions within 15 arcmin around V2493 Cyg.

The observational material comes from (i) the whole photographic plate stack preserved at Asiago Observatory (Italy) and the National Astronomical Observatory Rozhen (Bulgaria); from (ii) digitized plates from the Palomar Schmidt telescope; and (iii) several scanned plates from the Schmidt telescope of the Byurakan Astrophysical Observatory (Armenia). The CCD photometric observations were performed with the 2 m RCC, the 50/70 cm Schmidt and the 60 cm Cassegrain telescopes of the National Astronomical Observatory Rozhen (Bulgaria) and the 1.3 m RC telescope of the Skinakas Observatory<sup>1</sup> of the Institute of Astronomy, University of Crete (Greece). More observational and technical details are given in Semkov et al. (2012). All frames were exposed through a set of standard Johnson-Cousins filters. All the data were analyzed using the

<sup>1</sup> Skinakas Observatory is a collaborative project of the University of Crete, the Foundation for Research and Technology – Hellas, and the Max-Planck-Institut für Extraterrestrische Physik.

**Table 2.** Photometric observations of V2493 Cyg field on different telescopes.

Observatory/Telescope	Medium	Nr. of observations	Time span
Asiago Schmidt 67/92 and 40/50	photogr. plates	198	30. 8. 1962.–18. 11. 1998.
Palomar Schmidt	photogr. plates	6	5. 7. 1954.–12. 9. 1994.
Byurakan Schmidt 100/130	photogr. plates	6	28. 8. 1973.–22. 6. 1977.
Rozhen Schmidt 50/70	photogr. plates	4	18. 6. 1980.–11. 1. 1991.
Rozhen Schmidt and Cass.	CCD	105	29. 10. 2000.–6. 3. 2013.
Skinakas 1.3 m	CCD	91	14. 6. 2000.–22. 9. 2012.
Rozhen 2 m RCC	CCD	35	1. 6. 1997.–4. 5. 2013.

**Table 3.** Photometric data and coordinates for  $\alpha\beta\gamma\delta\epsilon\theta\omega\pi$  extended sequence stars taken from the NOMAD catalog.

Star	Nomad ID	$\alpha$ (J2000.0)	$\delta$ (J2000.0)	$B$	$V$	$R$	$I$	$B, V$ source	$R$ source
$\alpha$	1338-0411236	20 58 11.50	+43 52 04.0	10.73	10.51	10.38	10.31	T	B
$\beta$	1338-0411046	20 57 54.63	+43 49 34.7	13.35	12.71	12.23	11.89	D	D
$\gamma$	1338-0411059	20 57 55.49	+43 49 54.5	13.24	13.23	12.91	12.47	Y	B
$\delta$	1338-0411656	20 58 47.80	+43 51 41.7	15.14	14.05	13.32	12.79	D	D
$\epsilon$	1339-0412470	20 58 52.60	+43 54 51.3	13.25	12.54	12.01	11.64	D	D
$\theta$	1339-0412599	20 59 01.21	+43 59 34.9	12.14	11.46	11.04	10.75	D	D
$\omega$	1339-0412565	20 58 58.68	+43 57 15.3	11.67	11.17	10.86	10.61	D	D
$\pi$	1340-0418334	20 58 55.66	+44 03 37.4	7.71	6.64	5.98	5.66	T	B

**Notes.** Sources of the values are defined as follows: B = USNO-B1.0 (Monet et al. 2003); Y = YB6 Catalog (USNO, unpublished); T = Tycho-2 Catalog (Hog et al. 2000); D = DR6 data from APASS (transformed from the SLOAN system to the Johnson-Cousins  $BVRI$ ).

same aperture, which was chosen as  $4''$  in radius, and the background annulus was from  $9''$  to  $14''$ .

A log of the observing periods and telescopes used is given in the Table 2. The time span covers almost 60 years, from 1954 to 2013. The total number of photometric measurements performed for all sample stars and in all photometric bands is over 12 400, from which come 2549 on archival photographic plates.

Magnitudes were estimated using the A to O comparison sequence of fifteen stars in the field around V2493 Cyg calibrated in  $BVRI$  by Semkov et al. (2010). The used comparison sequence worked perfectly, covering the range of variability of the program stars, except for the V521 Cyg, which was brighter than comparison sequence stars. We then searched Nomad catalog and extended the comparison sequence with an additional eight bright stars of constant brightness called  $\alpha\beta\gamma\delta\epsilon\omega\theta\pi$  (corresponding photometric data is listed in Table 3, with noted sources of magnitudes). The finding chart for program and comparison sequence stars is given in Fig. 1.

The plates from Asiago Schmidt telescope were inspected visually using a high-quality Carl Zeiss microscope, which offered a variety of magnifications (Munari et al. 2001). The magnitude was then derived by comparing the variable with the stars in the same photometric sequence adopted for reducing of the CCD observations. We estimated the brightness of the variable  $V$  on photographic plates using  $a$  and  $b$ , two stars in the sequence where  $a$  is slightly brighter and  $b$  slightly fainter than  $V$ . The difference in brightness between  $a$  and  $b$ , as perceived by visually inspecting with a microscope, is divided into ten steps, and the difference in magnitude between  $V$  and the two stars is counted in terms of these steps, as  $n1$  and  $n2$ , conventionally expressed as “ $a n1 V n2 b$ ”, with  $n1 + n2 = 10$ . The magnitude of the variable  $V$  is then obtained from arithmetic proportion using known magnitudes of calibration sequence stars  $a$  and  $b$ .

Magnitude errors of archival plates measurements range from 0.03 to 0.20 most often taking the value 0.10. Errors are estimated by considering both the plate quality and the difference in magnitudes between two particular comparison sequence stars

chosen for magnitude estimation of the variable. Also, variable and comparison stars do not always lie in the plate center but sometimes on its edge, which diminishes accuracy in magnitude determination and is indicated by a higher error value.

Johnson and Cousins photometric systems (Johnson & Morgan 1953; Cousins 1976) were originally defined as photoelectric systems. Their details, passbands, and relation to many other photometric systems are reviewed at length in the Asiago Database of Photometric Systems (Moro & Munari 2000; Fiorucci & Munari 2003). Their porting to CCD detectors was discussed, among others, by Bessell (1990), while photographic realization were studied by Bell (1972) and Bessell (1979). Many different types of ortho- and pan-chromatic, as well as red and near-IR sensitive plates, have been used over the years at different observatories to carry out sky patrols. Adding to the varieties of combinations are the filters, which are from different manufacturers even if broadly similar in their transmission profiles. A posteriori there is not much a user can do in dealing with the emulsion-filter combination used to expose any given plates. Either the combination was close to a standard one (for example, both the 103a-D or Tri-X emulsion and GG11 or GG14 filters were valid choices in selecting the  $V$  band), and thus the plates can be measured against the proper local photometric sequence or the combination is too far off any valid one so the plate is ignored. The only exception is for the  $B$  band. The standard combination is 103a-O + GG13. However, for red objects, with a  $U - B > 1$ , an unfiltered 103a-O plate is still a valid substitute for a properly filtered one in realizing the  $B$  band.

### 3. Results and discussion

Measured Johnson-Cousins  $B, V, R_C, I_C$  magnitudes of program stars are given in Tables 4 and 5 and presented in Fig. A.1 for the whole observational period. Tables 4 and 5 are published in their entirety at the CDS. A small portion of each table is shown in the printed version of the article for guidance regarding its form and content. We deal with individual objects in Fig. A.1.

**Table 4.** Observations of the program stars from archive photographic plates.

Date	UT	Exposure	Magnitude	Error	HJD	Emulsion	Filter	Plate and telescope	Observatory
10 07 1967	00 50	60	$R = 12.28$	0.10	2 439 681.536	103a E	RG 1	741 Schmidt 67/92	Asiago
31 07 1971	00 54	20	$B = 12.55$	0.10	2 441 163.540	103a O	GG 13	4528 Schmidt 67/92	Asiago
18 09 1971	21 43	20	$V = 12.16$	0.10	2 441 213.407	TRI X	GG 14	9022 Schmidt 40/50	Asiago
24 08 1981	23 55	30	$B = 12.44$	0.10	2 444 841.500	103a O	GG 13	11084 Schmidt 67/92	Asiago
02 08 1989	00 45	30	$I = 11.70$	0.10	2 447 740.534	IN	RG 5	14580 Schmidt 67/92	Asiago
.....									

**Notes.** The full table is available at the CDS. A small portion of data for the star [KW 97] 53-36 is shown here for guidance regarding its form and content.

**Table 5.** CCD observations of the program stars.

Date	JD (-2 400 000)	$I$	err $_I$	$R$	err $_R$	$V$	err $_V$	$B$	err $_B$	Tel	CCD	Observatory
1997 Jun. 01	50 601.491	15.07	0.01	16.44	0.02	17.64	0.02	19.26	0.04	2 m	Phot	Rozhen
2003 Sep. 27	52 910.375	15.04	0.01	16.50	0.02	17.75	0.03	18.96	0.14	Sch	ST8	Rozhen
2008 Jun. 28	54 646.366	15.02	0.01	16.46	0.01	17.61	0.01	19.21	0.02	1.3 m	ANDOR	Skinakas
2010 Oct. 30	55 500.215	14.89	0.01	16.13	0.01	17.49	0.01	19.15	0.02	2 m	VA	Rozhen
2012 Aug. 13	56 152.624	14.96	0.02	16.32	0.03	17.36	0.04	18.76	0.13	1.3 m	ANDOR	Skinakas
.....												

**Notes.** The full table is available at the CDS. A small portion of data for the star V1716 Cyg is shown here for guidance regarding its form and content.

**Table 6.** Mean photometrical magnitudes and corresponding standard deviations for program stars.

Program star identifier	Mean magnitudes							
	$\langle B \rangle$	$\sigma_B$	$\langle V \rangle$	$\sigma_V$	$\langle R \rangle$	$\sigma_R$	$\langle I \rangle$	$\sigma_I$
[KW 97] 53-11	/	/	/	/	18.72	0.27	16.18	0.10
[KW 97] 53-17	/	/	19.26	0.52	17.66	0.32	15.29	0.36
[KW 97] 53-36	12.98	0.49	12.22	0.14	11.88	0.08	11.62	0.13
[KW 97] 53-20	19.82	0.39	17.85	0.36	16.27	0.30	14.42	0.30
[KW 97] 53-22	/	/	19.50	0.26	17.61	0.28	15.57	0.24
[KW 97] 53-23	20.39	0.44	18.47	0.24	16.85	0.20	14.94	0.17
EM* LkH $\alpha$ 186	18.14	1.06	16.67	0.90	15.51	0.74	14.20	0.54
EM* LkH $\alpha$ 187	19.24	0.29	17.56	0.35	16.21	0.23	14.69	0.16
EM* LkH $\alpha$ 189	18.19	0.22	16.50	0.20	15.28	0.15	13.97	0.14
EM* LkH $\alpha$ 191	14.01	0.19	12.91	0.08	12.21	0.07	11.65	0.14
V* V521 Cyg	14.80	0.42	13.73	0.25	12.94	0.22	12.09	0.17
V* V752 Cyg	17.43	0.65	16.64	0.54	15.86	0.41	14.88	0.28
V* V1538 Cyg	18.29	0.26	16.97	0.17	16.03	0.14	14.96	0.12
V* V1539 Cyg	16.92	0.17	15.54	0.12	14.49	0.09	13.51	0.10
V* V1716 Cyg	18.95	0.40	17.44	0.29	16.34	0.18	14.96	0.15
V* V1957 Cyg	17.38	0.14	16.20	0.10	15.38	0.09	14.54	0.07
V* V2051 Cyg	18.08	0.18	16.63	0.13	15.45	0.08	13.97	0.12

Mean magnitudes and corresponding standard deviations of program stars are given in Table 6. When the brightness of the variable is fainter than archival plate limiting magnitude, exact estimation of the magnitude is not possible. In such cases the magnitude of the last visible comparison sequence star was denoted as value “fainter than”.

The  $B - V$ ,  $V - R$ , and  $R - I$  color indices for all program stars in the whole observational period are presented in Fig. 2. They were calculated in all cases where the difference in the observational time for two bands was less than 24 h. To obtain measure of dispersion of the magnitudes, mean color indices  $B - V$ ,  $V - R$ , and  $R - I$  were calculated. Calculation did not include photographic measurements from the plates with only limiting magnitudes estimated. Mean color indices and corresponding standard deviations for program stars are given in Table 7, where it can be seen that  $B - V$  mean values for the stars [KW 97] 53-20

and [KW 97] 53-23 have standard deviations greater than 0.2. Possible causes of these values are discussed in the relevant star sections.

For all 17 program stars, we have reconstructed their photometric history from historical photographic plates and supplemented it by CCD observations in the Johnson-Cousins  $BVRI$  bands that cover the past 13 years. The total time span covered by our data is 60 years and for most all program stars represents first long-term photometric monitoring of the objects on a timescale of six decades. Recent CCD data have been used for a periodicity search of the program stars. Period analysis used the software package *PerSea*, version 2.6, based on a fast and statistically optimal period search in uneven sampled observations method by Schwarzenberg-Czerny (1996). The engine is based on the code from ISIS (image subtraction package) by Alard (2000). The classification algorithm was based on

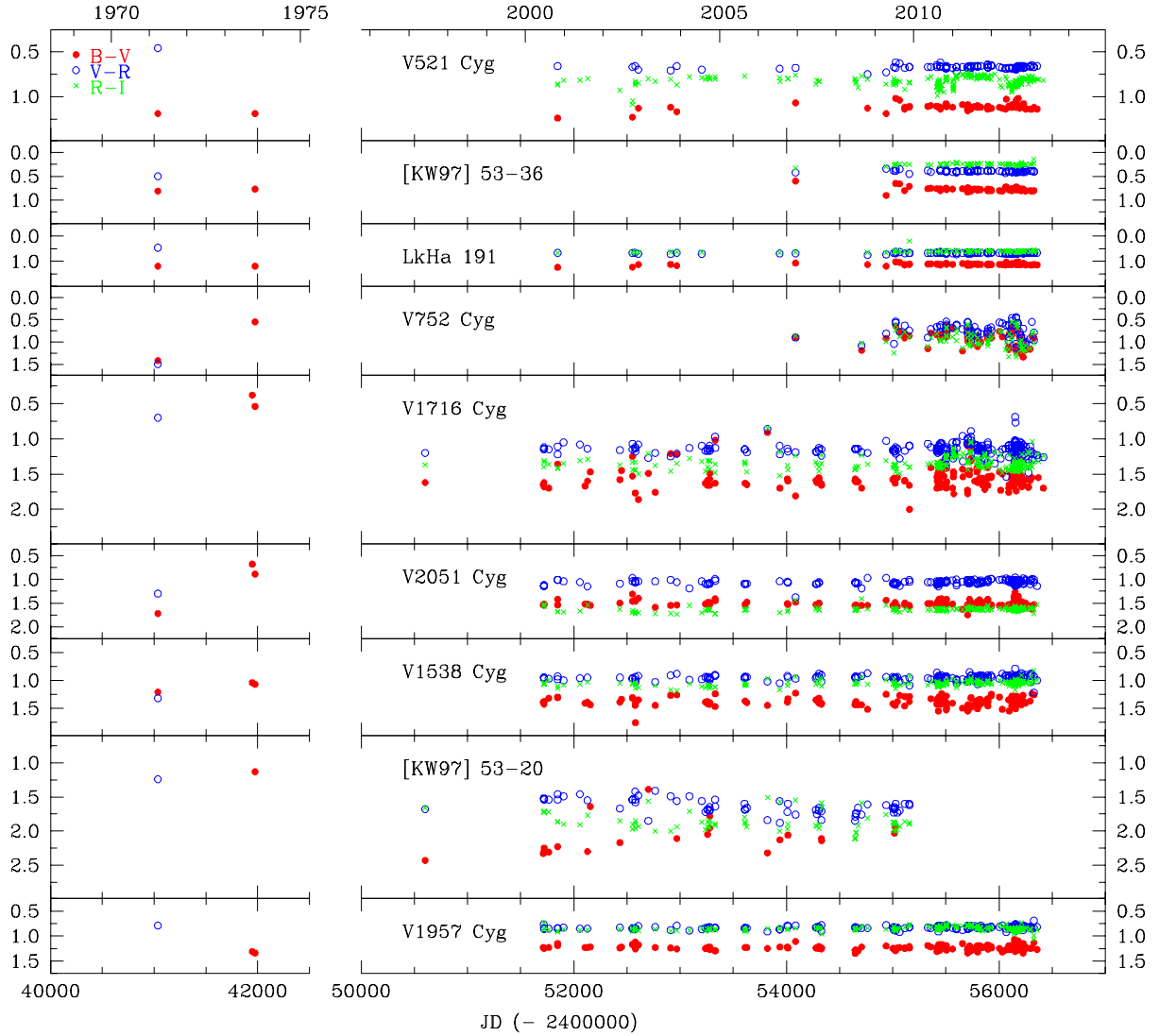


**Fig. 2.**  $B - V$ ,  $V - R$ , and  $R - I$  color indices for program stars.

Maciejewski & Niedzielski (2005). Additionally, periods were determined with *SygSpec* based on the theoretical concept introduced by (Reegen 2004, 2007). To estimate the false alarm probability (FAP), we randomly deleted 10% of our data 50 times and reran the period determination. As a measure of FAP confidence level, we calculated dispersion of this distribution.

We discuss each of the sample stars individually by extracting data from the references available since 1850, noticing specific points in the lightcurve and comparing them with already published photometric details. With this we assume that constant luminosity stars are those whose measurements are scattered just by errors, i.e. with amplitude of magnitudes lower than 0.20 mag (maximum error of individual measurements) and take an amplitude of magnitudes higher than 0.20 mag as an indicator of possible variability.

### 3.1. [KW 97] 53-11

The star [KW 97] 53-11 is mentioned in the catalog Kohoutek & Wehmeyer (1997, 1999) with brightness in the visual or photovisual colour system  $m_{pv} = 17^m20$ . Cohen & Kuhi (1979) provide near-infrared observations. The  $V$  magnitude was determined to

be  $V = 17^m20$  and the spectrum of the star estimated as M2. Armond et al. (2011) report a lack of  $H\alpha$  emission from this star.

In our measurements of  $B$  and  $V$  magnitudes, only determination of “fainter than” values was possible, and  $V$  values agree with the catalog data of the star; estimation of  $B$  values is given for the first time in this work, suggesting values below  $18^m00$  for a time interval of 50 years. The  $R$  values show slight scatter around  $18^m72$ , and  $I$  obtained from CCD measurements is fairly constant at  $16^m18$  (Table 6 and Fig. A.1).

### 3.2. [KW 97] 53-17, [KW 97] 53-20, and [KW 97] 53-22

The objects [KW 97] 53-17, [KW 97] 53-20, and [KW 97] 53-22 are mentioned in the Kohoutek & Wehmeyer (1997, 1999) catalog with only equatorial coordinates and finding charts available. Cohen & Kuhi (1979) provide near-infrared observations. Our measurements provide first-ever determinations of  $BVRI$  magnitudes. The position of all three stars is very close to the FUor V2493 Cyg, where they are submerged in the variable nebula stationed around the V2493 Cyg. Since V2493 Cyg from 2010 entered into outbursts, we exclude photometric measurements after 2010 from consideration in order to avoid the added light from the nebula and the variable background.

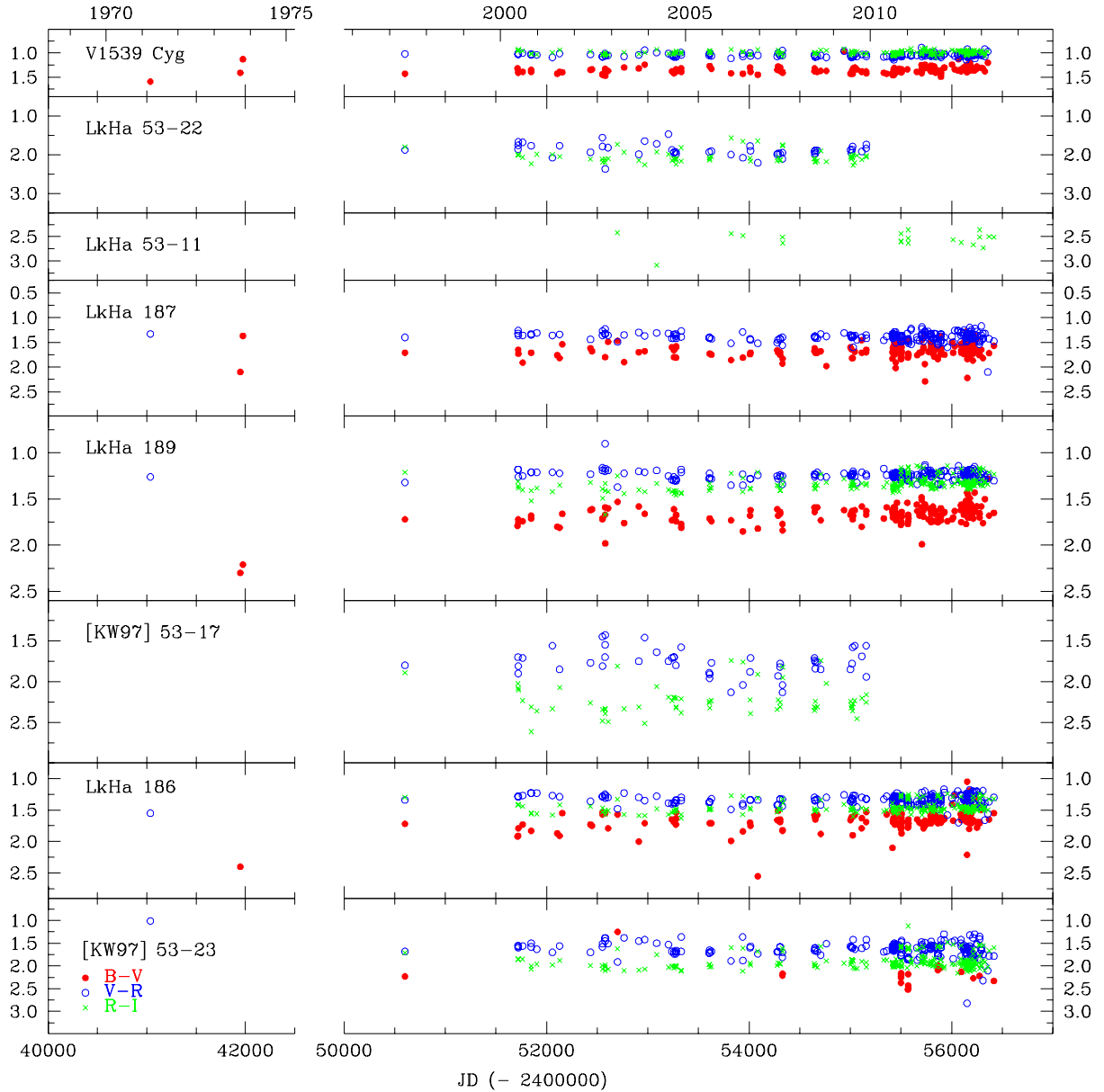


Fig. 2. continued.

For  $B$  magnitudes of the [KW 97] 53-17, only determination of “fainter than” values was possible, suggesting  $B$  less than  $18^m00$  in almost the whole time span. Mean magnitudes in our determinations are  $V = 19^m26$ ,  $R = 17^m66$ , and  $I = 15^m29$ , and in all bands they exhibit variations within 1 mag (Table 6 and Fig. A.1).

The star [KW 97] 53-20 also shows magnitude variations in all bands of about 1 mag and the mean magnitude values  $B = 19^m82$ ,  $V = 17^m85$ ,  $R = 16^m27$ , and  $I = 14^m42$  (Table 6 and Fig. A.1). In Table 7 a larger standard deviation of the mean  $B - V$  color index is evident. It arises mostly from a  $B - V$  value of 1.13 obtained from Asiago archive plates recorded on 1973 October 18. From Table 4 is evident that  $B$  value is less confident measurement since emulsion and filter combination of the plate are only the closest but not the exact  $B$  band.

Exact determination of  $BVRI$  magnitudes for the star [KW 97] 53-22 was not possible on the archive plates, while CCD measurements for the first time determine the mean magnitudes  $V = 19^m50$ ,  $R = 17^m61$ , and  $I = 15^m57$ . The  $B$  magnitudes

of the [KW 97] 53-22 only allowed determination of “fainter than” values, suggesting that  $B$  is less than  $18^m00$  in almost the whole time span (Table 6 and Fig. A.1).

Low amplitudes of variability and relatively stable light variations on a timescale of several decades for all three stars suggest WTTS behavior, most probably of Type I.

### 3.3. [KW 97] 53-36

One of the brightest stars in the sample is mentioned in the catalog Kohoutek & Wehmeyer (1997, 1999) with brightness in the photographic color system  $m_{pg} = 12^m70$ .

Our mean value of  $B = 12^m98$  is within  $\sigma$ , in accordance with this previous measurement by Kohoutek & Wehmeyer (1997). For the first time, we have determined mean values of  $V = 12^m22$ ,  $R = 11^m88$ , and  $I = 11^m62$  and monitored the star in a time span of six decades (Table 6 and Fig. A.1). Besides some larger scatter of measurements in archive data in comparison with those of CCD measurements, the star does not show

**Table 7.** Mean color indices and standard deviations for program stars.

Program star identifier	Mean color indices					
	$\langle B - V \rangle$	$\sigma_{B-V}$	$\langle V - R \rangle$	$\sigma_{V-R}$	$\langle R - I \rangle$	$\sigma_{R-I}$
[KW 97] 53-11	/	/	/	/	2.56	0.16
[KW 97] 53-17	/	/	1.77	0.16	2.22	0.19
[KW 97] 53-36	0.77	0.04	0.40	0.07	0.25	0.02
[KW 97] 53-20	2.05	0.32	1.63	0.12	1.86	0.13
[KW 97] 53-22	/	/	1.89	0.16	2.05	0.15
[KW 97] 53-23	2.18	0.26	1.63	0.17	1.90	0.16
EM* LkH $\alpha$ 186	1.66	0.17	1.34	0.08	1.46	0.08
EM* LkH $\alpha$ 187	1.68	0.14	1.39	0.09	1.53	0.10
EM* LkH $\alpha$ 189	1.66	0.11	1.24	0.05	1.33	0.07
EM* LkH $\alpha$ 191	1.12	0.04	0.67	0.03	0.60	0.05
V* V521 Cyg	1.26	0.06	0.84	0.04	0.83	0.05
V* V752 Cyg	0.91	0.18	0.76	0.18	0.93	0.19
V* V1538 Cyg	1.38	0.08	0.96	0.05	1.05	0.05
V* V1539 Cyg	1.35	0.07	1.04	0.04	0.99	0.03
V* V1716 Cyg	1.55	0.19	1.15	0.09	1.35	0.09
V* V1957 Cyg	1.24	0.06	0.83	0.03	0.85	0.04
V* V2051 Cyg	1.50	0.10	1.06	0.05	1.63	0.04

larger magnitude variations in the observed time span. Low amplitudes of variability and relatively stable light variations on a timescale of several decades of the star suggest a T Tauri variable star, possibly WTTS, type I.

### 3.4. [KW 97] 53-23

The star [KW 97] 53-23 is mentioned in the [Kohoutek & Wehmeyer \(1997, 1999\)](#) catalog with only equatorial coordinates and finding charts available. [Cohen & Kuhl \(1979\)](#) provide near-infrared observations.

We provide for the first time *BVRI* magnitudes of this faint object; mean values are  $B = 20^m39$ ,  $V = 18^m47$ ,  $R = 16^m85$ , and  $I = 14^m94$  (Table 6). From Table 7 it can be seen that the standard deviation for the mean  $B - V$  value of the star is slightly more than 0.2. There is not enough evidence that the cause could be some kind of star activity (flares), but it probably arise from statistical uncertainties in magnitude estimations. Long-term photometry of the star in a time span of six decades gives evidence of magnitude variations within 1 mag in all measured bands (Table 6 and Fig. A.1), suggesting that the object is probable a TTS.

### 3.5. LkH $\alpha$ 186 and LkH $\alpha$ 187

LkH $\alpha$  186 and LkH $\alpha$  187 were discovered by [Herbig \(1958\)](#) as H $\alpha$  emission line stars with weak H $\alpha$  intensity. In [Herbig & Bell \(1988\)](#), they are classified as T Tauri stars with photographic magnitudes  $m_{pg} = 18^m1$  and  $m_{pg} = 18^m0$  and spectral types K3 and K5 (respective to the star numbering). In [Cohen & Kuhl \(1979\)](#), infrared broad-band observations (out to at least  $3.5 \mu\text{m}$ ) and  $V$  magnitudes are provide  $V = 18^m1$ ,  $V = 18^m0$ . [Weaver & Jones \(1992\)](#) provide IRAS flux values. In [Kohoutek & Wehmeyer \(1997\)](#) brightness in the visual or photovisual color system ( $m_{pv} = 18^m1$ ,  $m_{pv} = 18^m0$ ) and spectral types K3IVe and K5IVe are given. [Ducourant et al. \(2005\)](#) have measured their proper motions. [Armond et al. \(2011\)](#) provide  $V$ ,  $R$ , and  $I$  magnitudes (LkH $\alpha$  186:  $V = 18^m12$ ,  $R = 16^m68$ ,  $I = 15^m85$ ; LkH $\alpha$  187:  $V = 18^m56$ ,  $R = 17^m05$ ,  $I = 16^m0$ ) and classify them as CTTS (class II).

Our determination of *BVRI* magnitudes indicates a brighter star for 1 mag in comparison with determination by [Armond et al. \(2011\)](#) in the case of both objects. Based on the data obtained from seven telescopes, our mean values are: LkH $\alpha$  186:  $B = 18^m14$ ,  $V = 16^m67$ ,  $R = 15^m51$ ,  $I = 14^m20$ ; LkH $\alpha$  187:  $B = 19^m24$ ,  $V = 17^m56$ ,  $R = 16^m21$ ,  $I = 14^m69$  (Table 6). Both stars show magnitude variations within 1 mag in the observed time interval in all measured bands with some larger scatter in archival data from photographic plates in  $I$  and  $V$  bands, possibly indicating variability in  $I$  of more than 1 mag (Fig. A.1). Our findings agrees with the classification of objects given by [Armond et al. \(2011\)](#) as CTTS stars.

LkH $\alpha$  186 in  $B$  band displays few events of a rise in brightness after 2011, possibly indicating burst activities (Table 6 and Fig. A.1).

### 3.6. LkH $\alpha$ 189

Discovered by [Herbig \(1958\)](#) as an H $\alpha$  emission line star with weak H $\alpha$  intensity, [Herbig & Bell \(1988\)](#) classified LkH $\alpha$  189 as a TTS with photographic magnitude  $m_{pg} = 17^m0$  and spectral type K6. [Cohen & Kuhl \(1979\)](#) carried out infrared broad-band observations (out to at least  $3.5 \mu\text{m}$ ), and  $V$  magnitude is provided  $V = 17^m0$ . [Weaver & Jones \(1992\)](#) provides IRAS flux values. In [Kohoutek & Wehmeyer \(1997\)](#), brightness in the visual or photovisual color system ( $m_{pv} = 17^m0$ ) and spectral type K6IVe is given. [Ducourant et al. \(2005\)](#) measured its proper motion. In [Laugalys et al. \(2006\)](#), the star is classified as T Tauri type star with  $V = 16^m69$  and spectral type K6. The position of LkH $\alpha$  189 in the two color  $J-H$  vs.  $H-K$  diagram obtained by the [Laugalys et al. \(2006\)](#) and [Meyer et al. \(1997\)](#) study of T Tauri properties using accretion disk models suggests increased disk thickness and interstellar reddening. [Corbally et al. \(2009\)](#) used LkH $\alpha$  189 SED for comparison with their sample stars SEDs. It is also mentioned in [Dobashi et al. \(1994\)](#) where astronomical objects are associated with molecular clouds. [Armond et al. \(2011\)](#) provide  $V = 17^m10$ ,  $R = 15^m80$ , and  $I = 15^m03$  and classify it as CTTS (class II).

Our measurements indicate the same range of  $V$  values as in [Armond et al. \(2011\)](#), [Cohen & Kuhl \(1979\)](#), [Kohoutek & Wehmeyer \(1997\)](#), and [Laugalys et al. \(2006\)](#), while mean

magnitude in  $I$  band is for about 1 mag less. The  $R$  band displays least scatter of measurements, which are in accordance with the data of [Armond et al. \(2011\)](#). The largest scatter is found in  $I$  band from 1990–1998 (Table 6 and Fig. A.1). This first-time long-term photometric behavior of the star suggests classification of the object as TTS (Fig. A.1).

### 3.7. LkH $\alpha$ 191

One of the best previous studied objects from the star sample, LkH $\alpha$ 191 was discovered by [Herbig \(1958\)](#) as an H $\alpha$  emission-line star with medium H $\alpha$  intensity. [Herbig & Bell \(1988\)](#) classified it as a TTS with photographic magnitude  $m_{pg} = 12^m.8$  and spectral type K0. In [Cohen & Kuhl \(1979\)](#), infrared broadband observations (out to at least  $3.5 \mu\text{m}$ ) were carried out, and  $V$  magnitude is  $V = 12^m.8$ . [Weaver & Jones \(1992\)](#) provides IRAS flux values. [Kohoutek & Wehmeyer \(1997\)](#) give brightness in the photoelectric  $V$  system ( $V = 13^m.0$ ) and spectral type K0Ve. [Ducourant et al. \(2005\)](#) measured its proper motion.

[Laugalys et al. \(2006\)](#) determined  $V = 13^m.06$  and spectral type K6e, noticed the absence of a strong H $\alpha$  emission and presence of only a small dust emission, and suggested no significant deviation of the star from the main sequence. The position of the star in their two-color  $J - H$  vs.  $H - K$  diagram is slightly below intrinsic T Tauri line. The authors conclude that LkH $\alpha$  191 has probably lost its envelope during the past 50 years ([Laugalys et al. 2006](#)). The SEDs of this object have been used by [Corbally et al. \(2009\)](#) for comparison with SEDs in their sample stars. [Valenti et al. \(1993\)](#) provide blue LkH $\alpha$  191 spectra. [Terranegra et al. \(1994\)](#) classify it as CTTS star and present  $uvby\beta$  photometry. [Fernandez et al. \(1995\)](#) classify it as the K0 TTS with  $V = 12^m.94$ . [Fernandez \(1995\)](#) presents the observational data of a photometric monitoring program carried out 1988–1992 in the  $UBV(RI)_C$  system with analysis of the variability and its possible origins discussed in [Fernandez & Eiroa \(1996\)](#). They report it as the constant object (with an amplitude in  $V$  from  $12^m.89$  to  $12^m.99$ ), with color index  $B - V$  in the range  $1^m.07 - 1^m.17$  and color index  $V - R$  in the range  $0^m.68 - 0^m.71$ . [Padgett \(1996\)](#) conducted a broad analysis of the spectra, determining the projected rotational velocities, equivalent width of temperature sensitive lines, effective temperature, microturbulent velocities, etc. In a long-term photometric variability of CTTS, [Grankin et al. \(2007\)](#) provide the  $V$  light curve of LkH $\alpha$  191 from July 1986 to August 1995 with  $V$  variations between  $12^m.87$  and  $13^m.09$ . They did not find any reliable dependence of  $V - R$  on  $V$  magnitude when averaged over all seasons. [Artemenko et al. \(2012\)](#) derived the periods and amplitudes of the rotational modulation of brightness and color as well as other rotational parameters. Our search for periodicity from CCD data could not confirm the findings of [Artemenko et al. \(2012\)](#). The reason lies probably in our observations, which are not dense enough to register the period. If dark spots on the surface of the star change positions very quickly, the rotational period cannot be recorded with a few observations per month.

The results of long-term photometry of LkH $\alpha$  191 given for the first time for a long time span are presented in Fig. A.1. Determined  $BVRI$  magnitudes fit those of [Grankin et al. \(2007\)](#) and [Fernandez & Eiroa \(1996\)](#) studies, showing similar values of  $V$  as well as color indices  $B - V$  and  $V - R$  (Tables 6 and 7). Data obtained in this work show scatter of about 1–1.5 mag in  $I$  and  $B$  bands, while those in  $R$  and  $V$  bands are even less, about 1 mag. The  $V$  magnitudes are fairly constant on the large time span. Our findings agree with the hypothesis of an CTTS star with no evidence of burst events in the past 60 years.

### 3.8. V521 Cyg

Another previously well studied object from the star sample, V521 Cyg was discovered by [Herbig \(1958\)](#) as an H $\alpha$  emission-line star with medium H $\alpha$  intensity. [Herbig & Bell \(1988\)](#) classified it as a TTS with photographic magnitude  $m_{pg} = 13^m.6$  and spectral type G8. In [Cohen & Kuhl \(1979\)](#), infrared broadband observations (out to at least  $3.5 \mu\text{m}$ ) were carried out. [Weaver & Jones \(1992\)](#) provide IRAS flux values. [Kohoutek & Wehmeyer \(1997\)](#) declare it to be a variable star with maximum brightness in the photoelectric  $V$  system ( $V = 13^m.6$ ) and spectral type K0. [Ducourant et al. \(2005\)](#) measured its proper motion. [Welin \(1973\)](#) confirmed it as H $\alpha$  emission-line star with medium H $\alpha$  intensity and determined  $B = 15^m.0$ ,  $V = 14^m.0$ , and it was presented as a variable star of RW Aurigae type. [Terranegra et al. \(1994\)](#) present  $uvby\beta$  photometry and classified the star as CTTS. [Fernandez et al. \(1995\)](#) provide and discuss the H $\alpha$  line profile. They classified the object as the G8 TTS with  $V = 13^m.6$ . [Herbst & Shevchenko \(1999\)](#) determined color indices  $B - V = 1^m.25$  and  $V - R = 1^m.18$ , average stellar magnitude  $V = 13^m.74$ , and the amplitude of its photometric activity  $\Delta V = 1^m.77$ . In [Mitskevich & Pavlenko \(2001\)](#), the light curve in the  $V$  band is shown. It is seen that for about 20 days (in August 1999), the star faded by 0.85 mag. [Ismailov \(2005\)](#) classify V521 Cyg as a type-V light curve representative star and provide the highest amplitude of light variations as  $\Delta V = 1^m.77$  and its light curve.

[Grankin et al. \(2007\)](#) conducted the long-term photometric variability of CTTS, providing  $V$  light curve of V521 Cyg from June 1986 to September 2003 with  $V$  variations between  $13^m.37 - 14^m.70$ . The star exhibits unusual color behavior with a blue turnaround at minimum brightness, arising possible from scattered light during partial occultation of the stellar photosphere by circumstellar material. Nonlinear dependence of  $V - R$  color index on  $V$  magnitude is present ([Grankin et al. 2007](#)).

[Laugalys et al. \(2006\)](#) classify V521 Cyg as a T Tauri type star with  $V = 13^m.66$  and spectral type K5. In their  $J - H$  vs.  $H - K$  diagram, the star is situated in the upper righthand corner, close to the intrinsic T Tauri line in the CTTS location. The properties of the TTS studied with the aid of accretion disk models suggest that the position of the star moved along the T Tauri line to larger color indices, and this is connected to an increase in disk thickness and to the strongest dust emission ([Meyer et al. 1997](#); [Laugalys et al. 2006](#)). [Corbally et al. \(2009\)](#) used V521 Cyg SED for comparison with their sample stars' SEDs. [Armond et al. \(2011\)](#) provide  $V = 14^m.65$ ,  $R = 13^m.69$ , and  $I = 13^m.37$  and classify it as a CTTS (class II). [Wenzel \(2011\)](#) provide 19 measurements of  $V$  magnitude from August to November 2010, ranging it from  $13^m.7$  to  $14^m.0$ .

Our measurements fit the amplitude of magnitudes determined in  $V$  band by [Mitskevich & Pavlenko \(2001\)](#) and [Grankin et al. \(2007\)](#). The light curve extends it to a longer time span and to  $I$  and  $R$  bands; mean magnitudes are  $B = 14^m.80$ ,  $V = 13^m.73$ ,  $R = 12^m.94$ , and  $I = 12^m.09$  (Table 6). Two declines in the beginning of 2002 are visible, one at the end of 2010 and the other in mid 2012 when star brightness faded for more than 1 mag (Table 6, Fig. A.1). These findings support the [Grankin et al. \(2007\)](#) hypothesis for earlier types of CTTS stars, possible UXor, with partial and irregular occultation of the stellar photosphere by circumstellar material as a cause of drops in the brightness of the star by one or more magnitudes. While there is a slight difference in mean values of  $V - R$  indices determined in this work compared to the values of [Herbst & Shevchenko \(1999\)](#), the mean values of  $B - V$  indices agree perfectly with

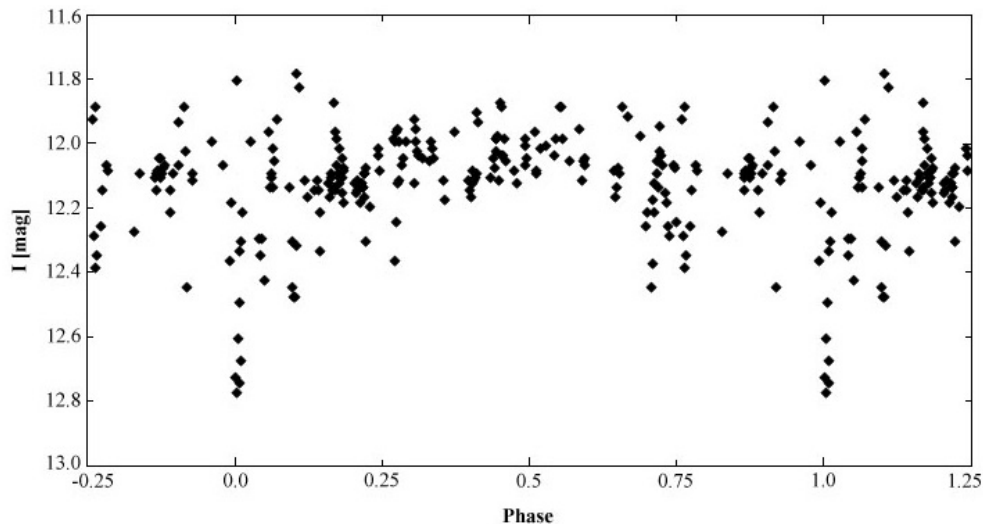


**Fig. 3.**  $I$  data of V521 Cyg folded onto a 503-day period.

relevant [Herbst & Shevchenko \(1999\)](#) determinations (Table 7 and Fig. 2).

The search for periodicity of V521 Cyg was fruitful: a period of 503 days has been found (Fig. 3) with the *PerSea* software package. Additionally, the period was also determined with *SygSpec*, which gave 519 days. Period analysis was done using our CCD data from the 2 m RCC, the 50/70 cm Schmidt, the 60 cm Cassegrain telescopes of the National Astronomical Observatory Rozhen (Bulgaria), and the 1.3 m RC telescope of the Skinakas Observatory of the Institute of Astronomy, University of Crete (Greece). The cause of the period found is probably precession of the circumstellar disk or eclipses from a second component or by clouds of gas and dust orbiting the star. FAP estimation was done by randomly deleting of 10% of data for 50 times and rerunning the period determination. As a measure of the FAP confidence level, we determined the dispersion of the period distribution arising from simulated data and obtained  $520 \pm 14$  days.

### 3.9. V752 Cyg

[Erastova & Tsvetkov \(1978\)](#) noted that the V752 Cyg behaves as a variable star, and they provide its finding chart. In [Kohoutek & Wehmeyer \(1997\)](#) brightness in photographic color system is given ( $m_{pg} = 15^m3$ ), corresponding to the maximum. They confirmed the variability of V752 Cyg and observed moderate  $H\alpha$  emission line and continuum.

We determined mean values of  $V = 16^m64$ ,  $R = 15^m86$ , and  $I = 14^m88$  for the first time and photometrically monitored the star in a longer time span (Table 6). Our observations confirm the variability of the star, which shows that the amplitude of magnitude variability in all bands increase from 1 mag in  $I$  up to 2.8 mag in  $V$  band (Fig. A.1). The relatively large amplitude of variability could also explain our mean value of  $B = 17^m43$ , which is about 2 mag greater than the value from previous measurements by [Kohoutek & Wehmeyer \(1997\)](#). Larger photometric amplitudes up to 2 or 3 mag, often irregular, could indicate the type II variability of CTTs, that is, the presence of short-lived accretion-related events on the stellar surface of CTTs ([Herbst 2012](#)). In mid 2012, V752 Cyg exhibited the largest variability amplitude in the past 60 years observed in all bands, especially in  $B$  and  $V$ .

### 3.10. V1538 Cyg

[Erastova & Tsvetkov \(1974\)](#) discovered V1538 Cyg as a flare star. [Corbally et al. \(2009\)](#) provide its spectrum and classify it as an M1 with low emission in  $H\alpha$ . The authors found no indications of any envelope, suggesting that the star can be either an unreddened field dwarf with chromospheric activity, located at 350 pc, or a post-TTS.

For the first time we have determined mean values of  $B = 18^m29$ ,  $V = 16^m97$ ,  $R = 16^m03$ , and  $I = 14^m96$  (Table 6). Our measurements indicate small magnitude variations (less than 0.5 mag) after 2000, and some larger scatter of the measurements before 2000 in the  $B$  and  $V$  bands (Fig. A.1). Low amplitudes of variability and relatively stable light variations on a timescale of several decades confirm the [Corbally et al. \(2009\)](#) assumption of a T Tauri or post T Tauri variable.

### 3.11. V1539 Cyg

V1539 Cyg was discovered by [Herbig \(1958\)](#) as an  $H\alpha$  emission line star with strong  $H\alpha$  intensity. In [Herbig & Bell \(1988\)](#), it is classified as TTS with photographic magnitude  $m_{pg} = 16^m3$  and spectral type K6. [Cohen & Kuhl \(1979\)](#) provided infrared broad-band observations (out to at least  $3.5 \mu\text{m}$ ) and  $V$  magnitude:  $V = 16^m3$ . [Weaver & Jones \(1992\)](#) provide IRAS flux values. [Kohoutek & Wehmeyer \(1997\)](#) declare it to be a variable star with maximum brightness in the photoelectric  $V$  system ( $V = 14^m5$ ) and spectral type K6IVe. [Ducourant et al. \(2005\)](#) measured its proper motion. [Welin \(1973\)](#) confirmed it as an  $H\alpha$  emission-line star with strong  $H\alpha$  intensity and determined  $B = 17^m0$  and  $V = 15^m5$ . [Giesekeing & Schumann \(1976\)](#) discovered that V1539 Cyg has light variations greater than 0.25, which led to the conclusion of the suspected variability.

[Laugalys et al. \(2006\)](#) classified it as an emission-line, T Tauri type variable with  $V = 15^m48$  and spectral class K6. In the two-color  $J - H$  vs.  $H - K$  diagram, the star is situated in the upper righthand corner, above the intrinsic T Tauri line, suggesting an increase in disk thickness or stronger dust emission ([Meyer et al. 1997](#); [Laugalys et al. 2006](#)). [Corbally et al. \(2009\)](#) provide spectral classification of V1539 Cyg as G5e. According to the SED, it is young stellar object of class II with considerable thermal emission from the dust envelope. [Armond et al. \(2011\)](#) provide  $V = 16^m22$ ,  $R = 15^m08$ , and  $I = 14^m60$  and

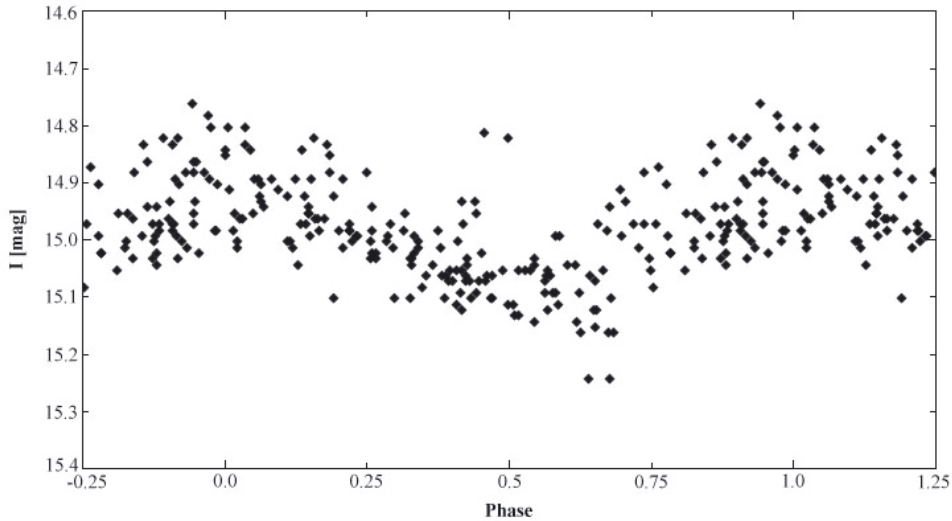


**Fig. 4.**  $I$  data of V1716 Cyg folded onto a 4.15-day period.

classify it as CTTS (class II). [Findeisen et al. \(2013\)](#) report an episode of brightening or a burster event of the object obtained from Palomar measurements from 2009 to 2013. The  $R$  magnitude estimation was 14.6 mag, and the lightcurve is described as first half of a 0.3 mag burst then a data gap in mid-2011 with rise time of two days.

Our measurements for V1539 Cyg (Table 6 and Fig. A.1) indicate accordance with the  $V$  and  $B$  values determined by [Welin \(1973\)](#) and the  $R$  values obtained by [Findeisen et al. \(2013\)](#). Obtained results in our long time photometric monitoring agree with star classification as a CTTS. Our measurements do not show evidence of other  $R$  brightening episodes, such as the one reported by [Findeisen et al. \(2013\)](#).

### 3.12. V1716 Cyg

It is listed as the 65th name in a list of the variable stars provided by [Kholopov et al. \(1981\)](#), but it was discovered and classified as a variable star for the first time in [Erastova & Tsvetkov \(1978\)](#). [Findeisen et al. \(2013\)](#) found two burst events of the object, separated by 35 days, first in July 2011 lasting 5 to 20 days and the second lasting 3 days. The mean  $R$  magnitude was  $16^m.5$ .

We determined mean values of  $B = 18^m.95$ ,  $V = 17^m.44$ , and  $I = 14^m.96$  (Table 6) and find a mean value of  $R = 16^m.34$ , in good agreement with the data of [Findeisen et al. \(2013\)](#). Our measurements confirm the variability of the star with magnitude amplitude of about 1 mag increasing toward the  $B$  band. The rise in brightness of V1716 Cyg in June 2011 observed by [Findeisen et al. \(2013\)](#) is evident from 0.5 mag in  $I$  up to 1.8 mag in  $B$  band. Our measurement indicates an eruptive event of V1716 Cyg in March 2006 that is observable in all bands (Fig. A.1). Moderate amplitude of variability leaning to a brightness-rise episodes indicate V1716 Cyg as a CTTS star, possibly type II.

A periodicity search using CCD data from recent years indicates a 4.15-day period that is stable in the time of several years (Fig. 4). The same period was obtained with *PerSea*, as well as with the *SygSpec* package. It is a typical rotational period for TTS. At the same time, we recorded two short flares of this star excluded from the periodicity analysis. Exclusion of the data from the outbursts of V1716 Cyg in the search for periodicity was necessary because these are two separate phenomena that cannot be linked. Flares in UV Cet type stars occur

in the stellar chromosphere. They are random events that are not related to the position of the dark spots on the stellar surface. FAP estimation was done by randomly deleting 10% of the data for 50 times and then rerunning the period determination. Dispersion of this distribution, which can be used as a measure of FAP confidence level was  $4.1539 \pm 0.0002$  days. The period determination remain stable, even with a subsample with 20% of the data removed.

### 3.13. V1957 Cyg

[Kazarovets & Samus \(1990\)](#) determined the range of variability in  $V$  from  $16^m.00$  to  $18^m.00$ . [Laugalys et al. \(2006\)](#) classified V1957 Cyg as a K dwarf with possible  $H\alpha$  emission. Its green Vilnius magnitude is  $V = 16^m.29$ , and its spectral class is K6. In [Corbally et al. \(2009\)](#), the spectrum of the star is provided, and it is assumed that it could be a reddened G main sequence star or M0V star.

We determined for the first time mean values of  $B = 17^m.38$ ,  $R = 15^m.38$ , and  $I = 14^m.54$  and presented photometric monitoring of the star on a longer time span (Table 6). The mean  $V = 16^m.20$  value agrees well with the value of [Laugalys et al. \(2006\)](#). Our measurements indicate small magnitude variations (less than 0.3 mag) after 2000, and slightly larger scatter of the measurements before 2000 (Fig. A.1). Low amplitude of variability and relatively stable light variations on a timescale of several decades confirm the assumptions on the nature of V1957 Cyg supposed by [Corbally et al. \(2009\)](#).

### 3.14. V2051 Cyg

[Parsamian et al. \(1994\)](#) discovered V2051 Cyg as a flare star. The [Kazarovets & Samus \(1997\)](#) range of variability in the  $V$  band from  $14^m.00$  to  $18^m.00$ . [Corbally et al. \(2009\)](#) provide the spectrum of V2051 Cyg and estimate its spectral class as M3.5e, with faint  $H\alpha$  emission noted. The authors suggest that the energy distribution of the star, constructed from the 2MASS and *Spitzer* observations, also gives evidence of a normal star without an envelope, most probably an M-dwarf with weak chromospheric activity. Its green Vilnius magnitude is  $V = 16^m.59$ .

Our measurements of mean  $V = 16^m.63$  fit the estimations of [Kazarovets & Samus \(1997\)](#) and [Corbally et al. \(2009\)](#) well.

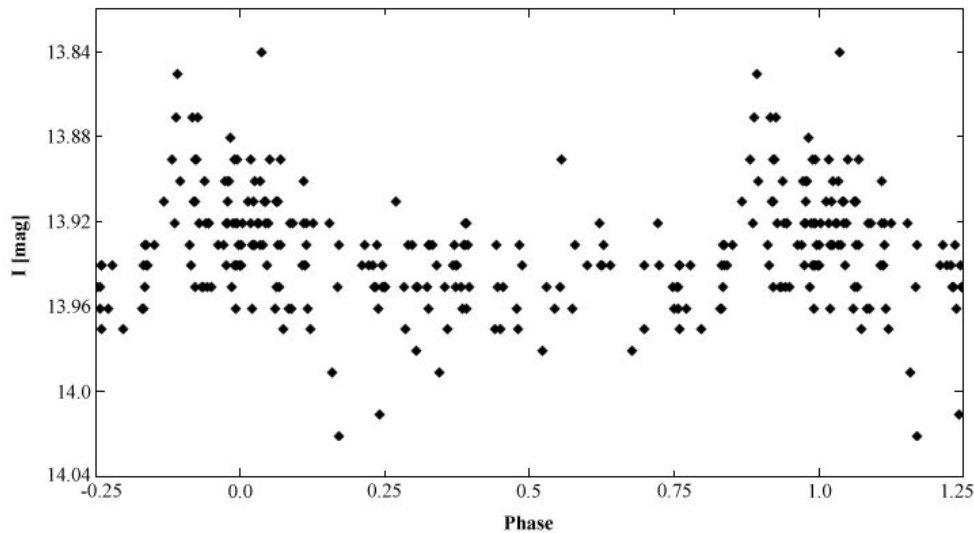


**Fig. 5.** *I* data of V2051 Cyg folded onto a 384-day period.

Magnitude variations of the star are less than 0.5 mag in the whole observational period. Mean values of  $B = 18^m08$ ,  $R = 15^m45$ , and  $I = 13^m97$  are determined (Table 6 and Fig. A.1). The low amplitude of variability and relatively stable light variations on a timescale of several decades confirm the assumptions on the nature of V2051 Cyg supposed by Corbally et al. (2009).

Search of periodicity using recent CCD data lead for the first time to determining a period of 384 days (Fig. 5) obtained with the *PerSea* and 372 days with the *SygSpec* package. As in the case of V521 Cyg, it could be caused by precession of the circumstellar disc by clouds of gas and dust orbiting the star. FAP estimation has been done by randomly deletion of 10% of data for 50 times and rerunning the period determination. As a measure of the FAP confidence level, we determined the dispersion of the obtained distribution as  $378 \pm 5$  days.

### 3.15. Concluding remarks

Our  $BVR_cI_c$  observations of V2493 Cyg zone cover 60-year time span and represents the first long-term photometry issued for 17 stars from the zone detected as  $H\alpha$  emission-line stars in Herbig (1958) and mostly classified as TTS. Our results complement the previously rare insights into their photometry and photometric history. Eight investigated objects are found to mostly be CTTS stars of type II variability, while for six of them we found indications of WTTS star mostly of variability type I. For three program stars, periodicities have been found for the first time; V1716 Cyg indicates 4.15-day period, V2051 Cyg indicates a 384 day period, and V521 Cyg a 503-day period. The LkH $\alpha$  191 periodicity could not be detected by our observations. The FAP estimation for three periods determinations was done with the software packages *PerSea*, Version 2.6, and *SygSpec* used for period analysis. We randomly deleted 10% of the data for 50 times and reran the period determinations. Dispersion of such obtained distribution was calculated as a measure of FAP confidence level. Further observations with spectroscopic measurements obtained simultaneously with photometric one, would offer clearer insight into the physical processes responsible for the observed variability of PMS stars.

*Acknowledgements.* We are indebted to Ulisse Munari for useful suggestions and helpful discussions during the elaboration of this work. We are grateful to Tomislav Terzić for the help and suggestions with numerical calculus. Thanks are

due to the anonymous referee for valuable comments and suggestions that improved the article. R.J.S. and I.P.B. thank the INAF Astronomical Observatory of Padova for the hospitality during the stay in Asiago and for permission to use the historical plate archive of Asiago Observatory. This work was supported in part by the University of Rijeka under the project number 13.12.1.3.03. This work was partly supported by ESF and the Bulgarian Ministry of Education and Science under contract BG051PO001-3.3.06-0047. The authors thank the Director of Skinakas Observatory, Prof. I. Papamastorakis, and Prof. I. Papadakis for granting telescope time. The Digitized Sky Survey was produced at the Space Telescope Science Institute under US Government grant NAG W-2166. The images of these surveys are based on photographic data obtained using the *Oschin* Schmidt Telescope on Palomar Mountain and the UK Schmidt Telescope. The plates were processed into the present compressed digital form with the permission of these institutions.

### References

- Alard, C. 2000, *A&AS*, 144, 363  
 Armond, T., Reipurth, B., Bally, J., & Aspin, C. 2011, *A&A*, 528, A125  
 Artemenko, S. A., Grankin, K. N., & Petrov, P. P. 2012, *Astron. Lett.*, 38, 783  
 Bell, R. A. 1972, *MNRAS*, 159, 357  
 Bessell, M. S. 1979, *PASP*, 91, 589  
 Bessell, M. S. 1990, *PASP*, 102, 1181  
 Cohen, M., & Kuhl, L. V. 1979, *ApJS*, 41, 743  
 Corbally, C. J., Straižys, V., & Laugalys, V. 2009, *Balt. Astron.*, 18, 111  
 Cousins, A. W. J. 1976, *MmRAS*, 81, 25  
 Dobashi, K., Bernard, J.-P., Yonekura, Y., & Fukui, Y. 1994, *ApJS*, 95, 419  
 Ducourant, C., Teixeira, R., Périé, J. P., et al. 2005, *A&A*, 438, 769  
 Erastova, L. K., & Tsvetkov, M. K. 1974, *IBVS*, 909, 1  
 Erastova, L. K., & Tsvetkov, M. K. 1978, *Peremennye Zvezdy*, 21, 79  
 Fernandez, M. 1995, *A&AS*, 113, 473  
 Fernandez, M., & Eiroa, C. 1996, *A&A*, 310, 143  
 Fernandez, M., Ortiz, E., Eiroa, C., & Miranda, L. F. 1995, *A&AS*, 114, 439  
 Findeisen, K., Hillenbrand, L., Ofek, E., et al. 2013, *ApJ*, 768, 93  
 Fiorucci, M., & Munari, U. 2003, *A&A*, 401, 781  
 Giesekeing, F., & Schumann, J. D. 1976, *A&AS*, 26, 367  
 Grankin, K. N., Melnikov, S. Y., Bouvier, J., Herbst, W., & Shevchenko, V. S. 2007, *A&A*, 461, 183  
 Grankin, K. N., Bouvier, J., Herbst, W., & Melnikov, S. Y. 2008, *A&A*, 479, 827  
 Green, J. D., Evans, II, N. J., Kóspál, Á., et al. 2011, *ApJ*, 731, L25  
 Herbig, G. H. 1958, *ApJ*, 128, 259  
 Herbig, G. H., & Bell, K. R. 1988, *Third Catalog of Emission-Line Stars of the Orion Population* (Santa Cruz: Lick Observatory)  
 Herbst, W. 2012, *Journal of the American Association of Variable Star Observers*, 40, 448  
 Herbst, W., & Shevchenko, V. S. 1999, *AJ*, 118, 1043  
 Herbst, W., Herbst, D. K., Grossman, E. J., & Weinstein, D. 1994, *AJ*, 108, 1906  
 Hog, E., Fabricius, C., Makarov, V. V., et al. 2000, *VizieR online data catalogue*, I/259  
 Ismailov, N. Z. 2005, *Astron. Rep.*, 49, 309  
 Johnson, H. L., & Morgan, W. W. 1953, *ApJ*, 117, 313  
 Joy, A. H. 1942, *PASP*, 54, 15

- Joy, A. H. 1945, *ApJ*, 102, 168
- Kazarovets, E. V., & Samus, N. N. 1990, *IBVS*, 3530, 1
- Kazarovets, E. V., & Samus, N. N. 1997, *IBVS*, 4471, 1
- Kholopov, P. N., Samus', N. N., Kukarkina, N. P., Medvedeva, G. I., & Perova, N. B. 1981, *IBVS*, 1921, 1
- Kohoutek, L., & Wehmeyer, R. 1997, *Abhandlungen aus der Hamburger Sternwarte*, Band 11, Teil 1, 2
- Kohoutek, L., & Wehmeyer, R. 1999, *A&AS*, 134, 255
- Kóspál, A., Ábrahám, P., Acosta-Pulido, J. A., et al. 2011, *A&A*, 527, A133
- Laugalys, V., Straizys, V., Vrba, F. J., et al. 2006, *Balt. Astron.*, 15, 483
- Leoni, R., Larionov, V. M., Centrone, M., et al. 2010, *ATel*, 2854
- Maciejewski, G., & Niedzielski, A. 2005, *Baltic Astron.*, 14, 205
- Ménard, F., & Bertout, C. 1999, in *The Origin of Stars and Planetary Systems*, eds. C. J. Lada, & N. D. Kylafis, *NATO ASIC Proc.*, 540, 341
- Meyer, M. R., Calvet, N., & Hillenbrand, L. A. 1997, *AJ*, 114, 288
- Miller, A. A., Hillenbrand, L. A., Covey, K. R., et al. 2011, *ApJ*, 730, 80
- Mitskevich, M. P., & Pavlenko, E. P. 2001, *Astrophysics*, 44, 411
- Monet, D. G., Levine, S. E., Casian, B., et al. 2003, *VizieR online data catalogue*, I/284
- Moro, D., & Munari, U. 2000, *A&AS*, 147, 361
- Munari, U., Jurdana-Šepić, R., & Moro, D. 2001, *A&A*, 370, 503
- Munari, U., Milani, A., Valisa, P., & et al. 2010, *ATel*, 2808
- Padgett, D. L. 1996, *ApJ*, 471, 847
- Parsamian, E. S., Chavira, E., & Gonzalez, G. 1994, *IBVS*, 4047, 1
- Reegen, P. 2004, in *The A-Star Puzzle*, *Proc. IAU Symp.* 224, eds. J. Zverko, J. Ziznovsky, S. J. Adelman, & W. W. Weiss, 791
- Reegen, P. 2007, *A&A*, 467, 1353
- Schwarzenberg-Czerny, A. 1996, *ApJ*, 460, L107
- Semkov, E. H., Peneva, S. P., Munari, U., Milani, A., & Valisa, P. 2010, *A&A*, 523, L3
- Semkov, E. H., Peneva, S. P., Munari, U., et al. 2012, *A&A*, 542, A43
- Terranegra, L., Chavarría-K., C., Diaz, S., & Gonzalez-Patino, D. 1994, *A&AS*, 104, 557
- Valenti, J. A., Basri, G., & Johns, C. M. 1993, *AJ*, 106, 2024
- Weaver, W. B., & Jones, G. 1992, *ApJS*, 78, 239
- Welin, G. 1973, *A&AS*, 9, 183
- Wenzel, K. 2011, *BAV Rundbrief – Mitteilungsblatt der Berliner Arbeitsgemeinschaft fuer Veraenderliche Sterne*, 60, 23

**Appendix A:  $BVR_cI_c$  magnitudes of the program stars**

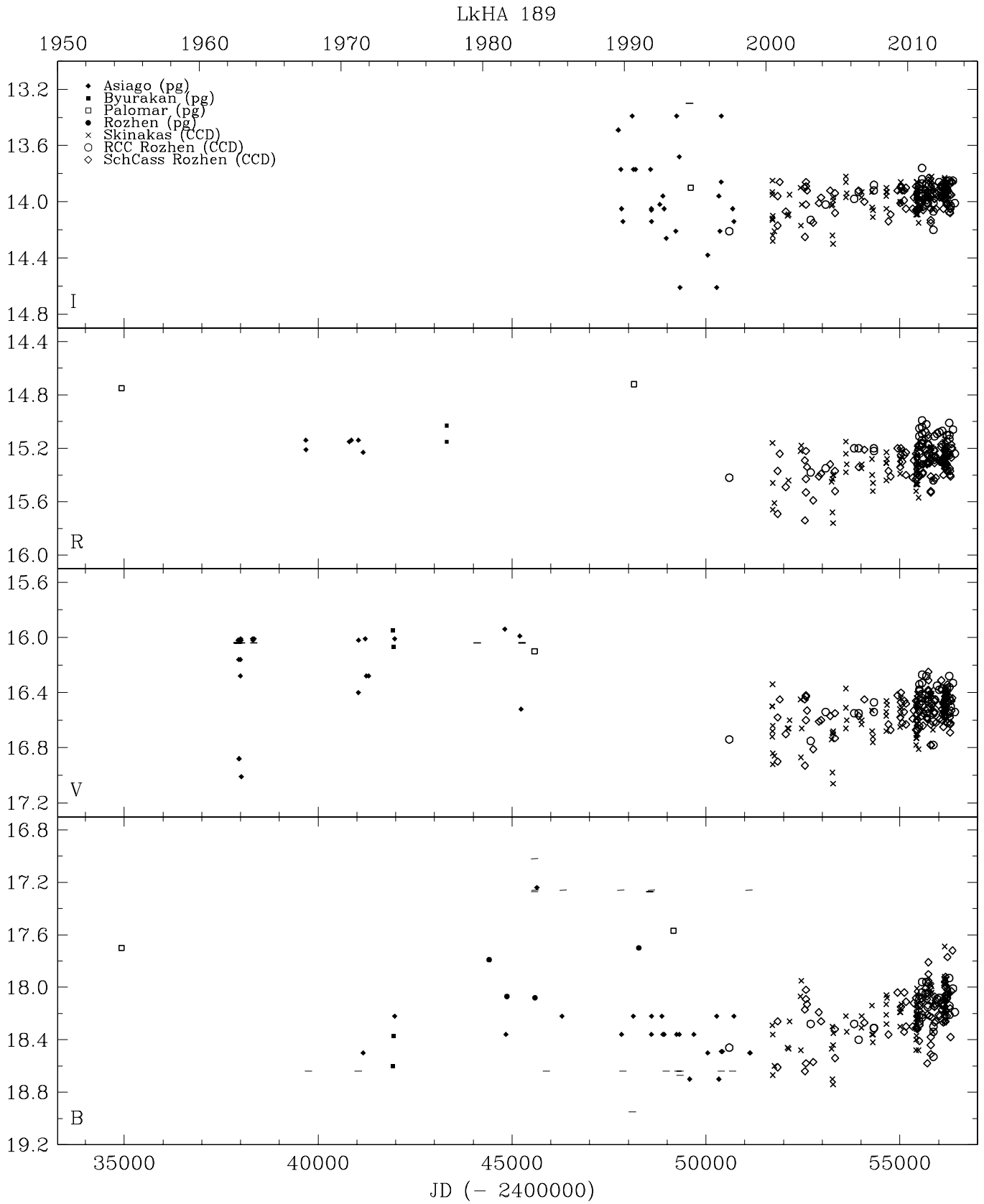


**Fig. A.1.**  $BVR_cI_c$  magnitudes of the program stars. (“-” symbol: fainter than).

[KW97] 53-11

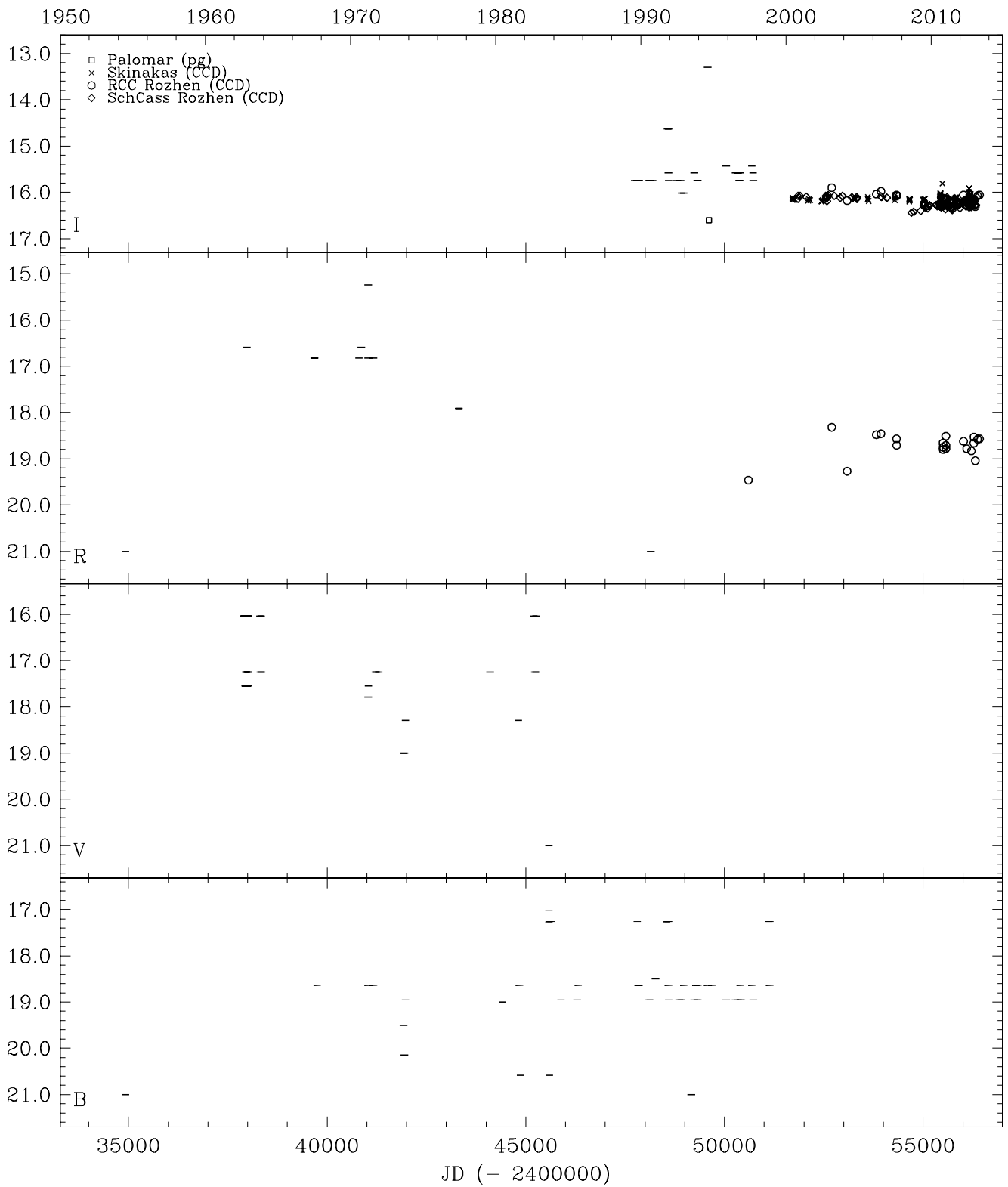


Fig. A.1. continued.

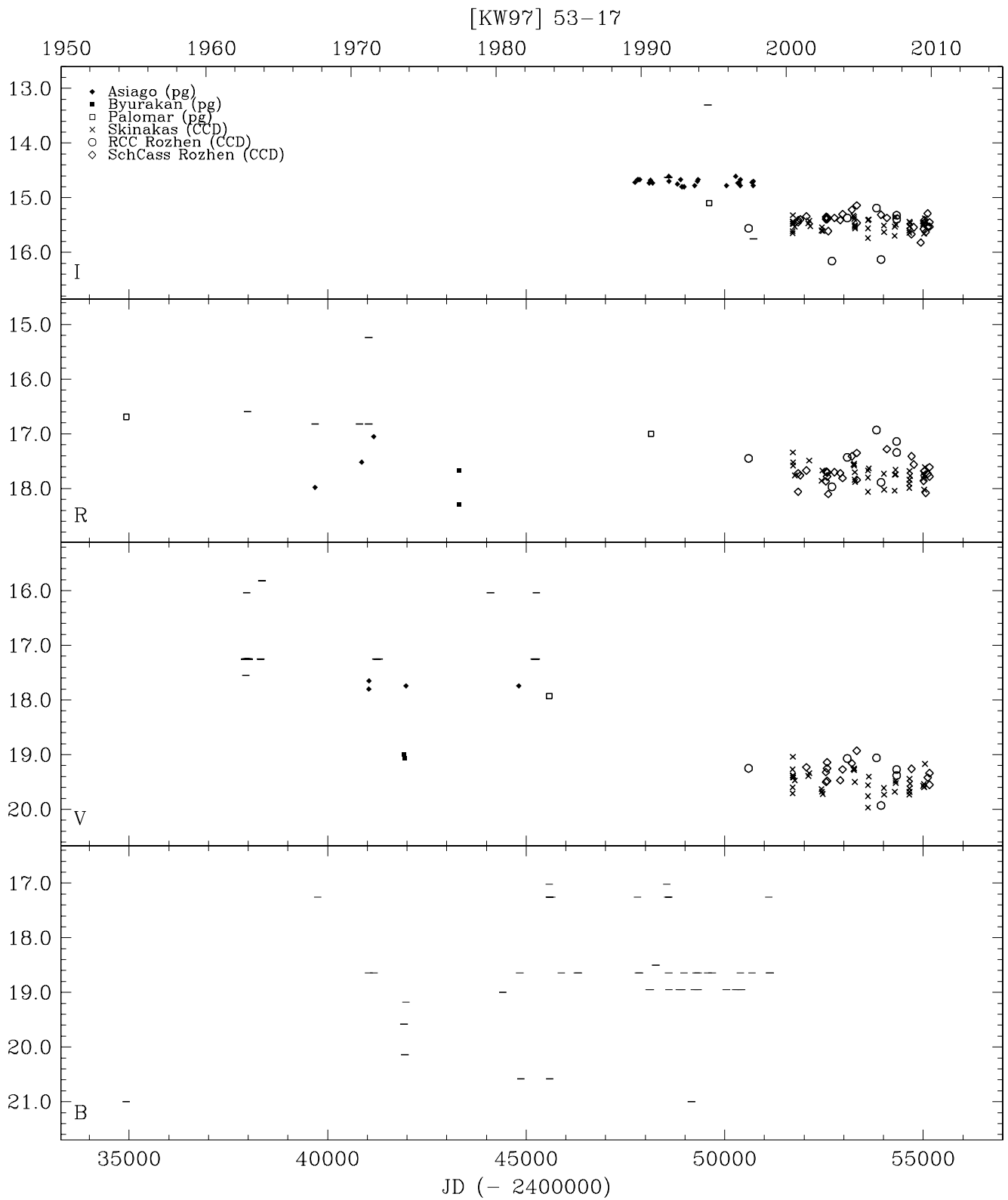


Fig. A.1. continued.

[KW97] 53-20

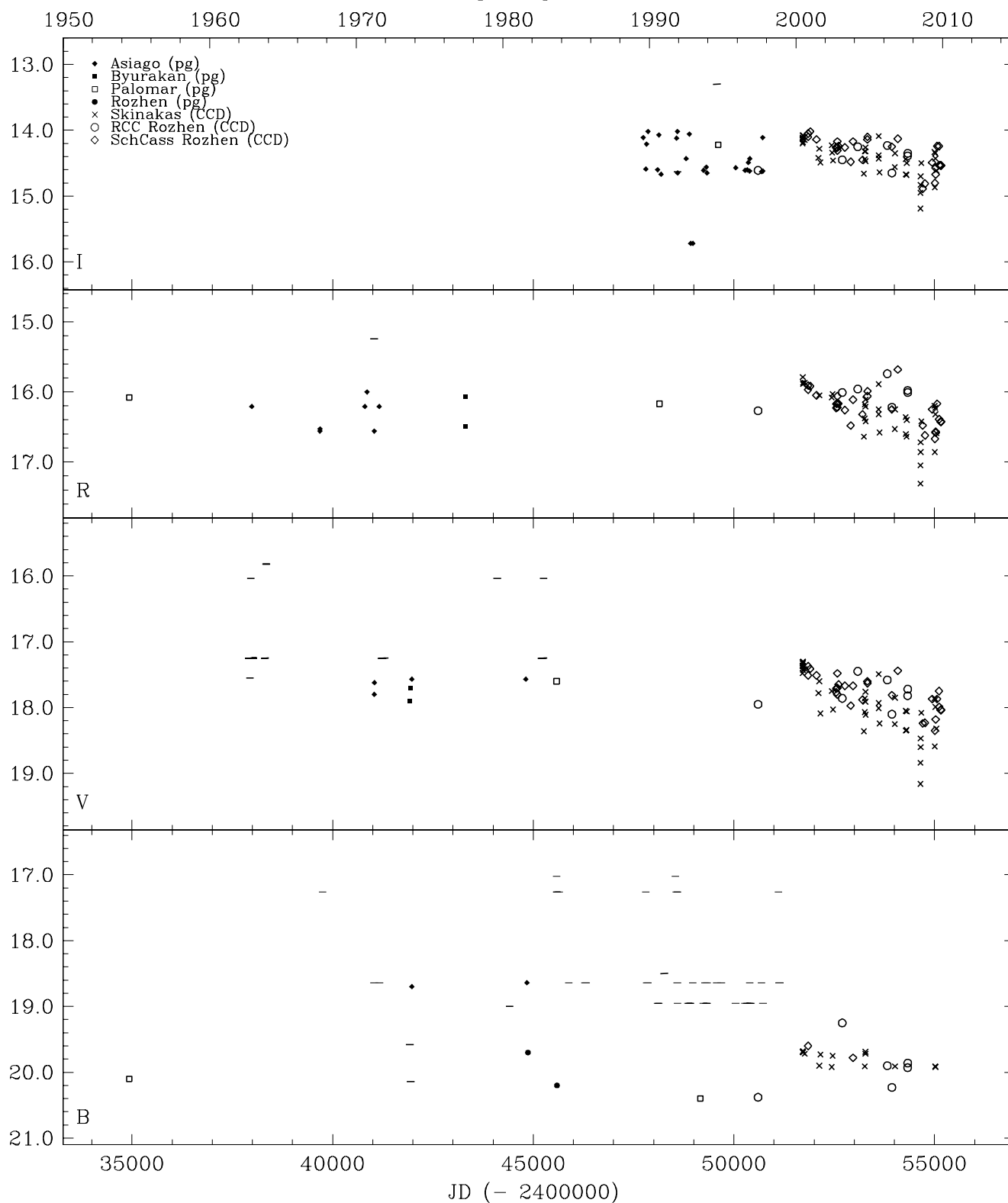


Fig. A.1. continued.

[KW97] 53-22

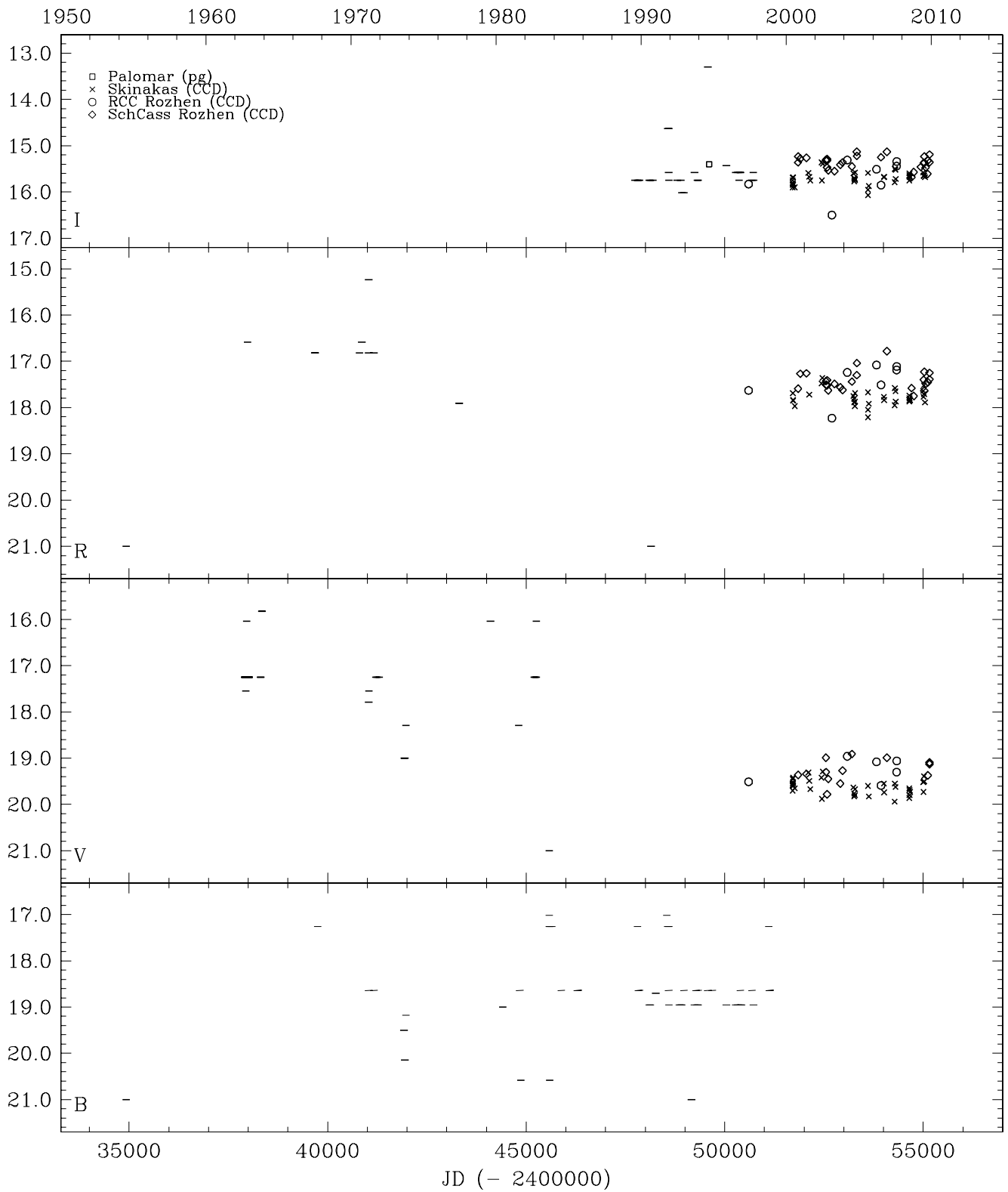


Fig. A.1. continued.

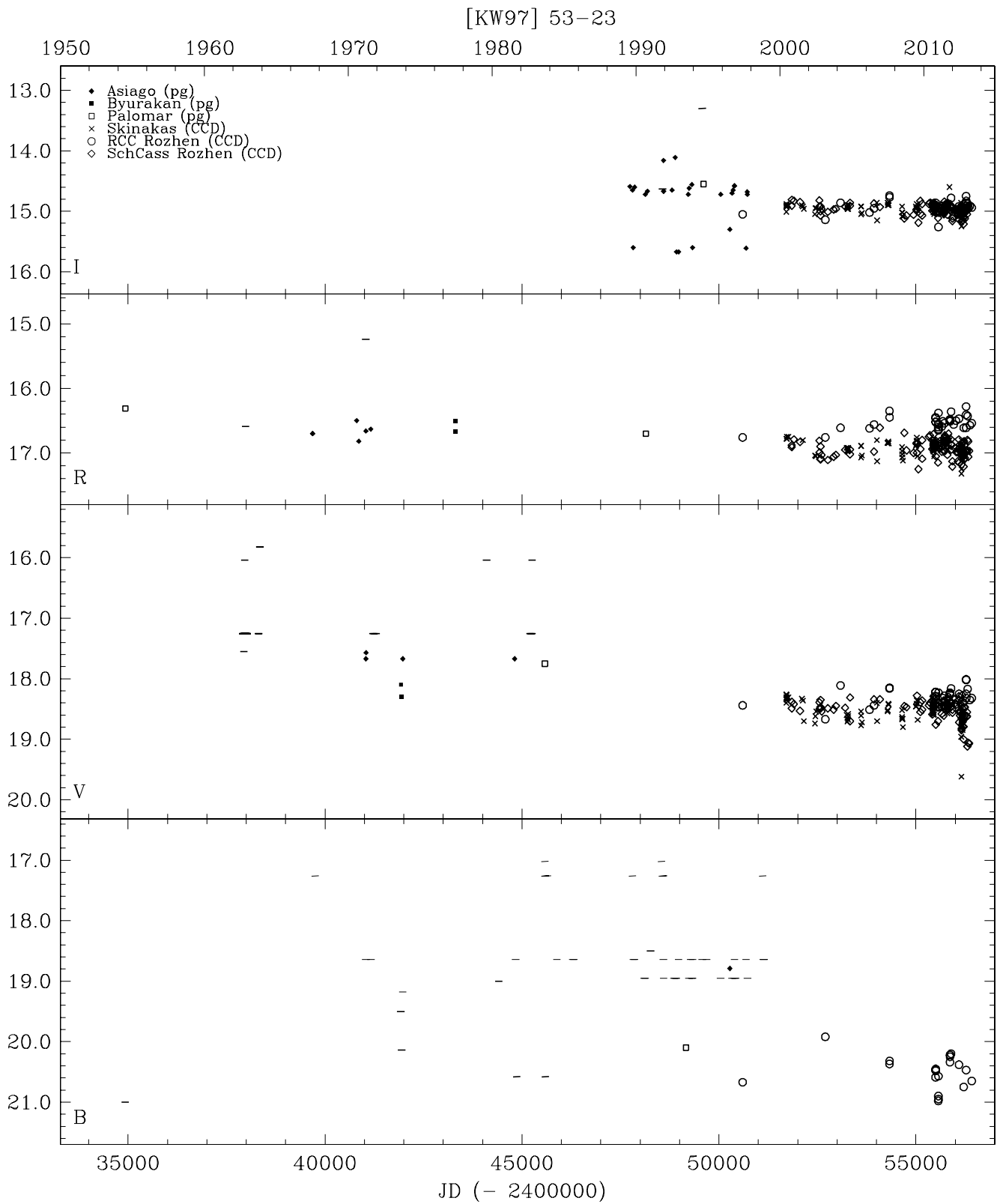


Fig. A.1. continued.

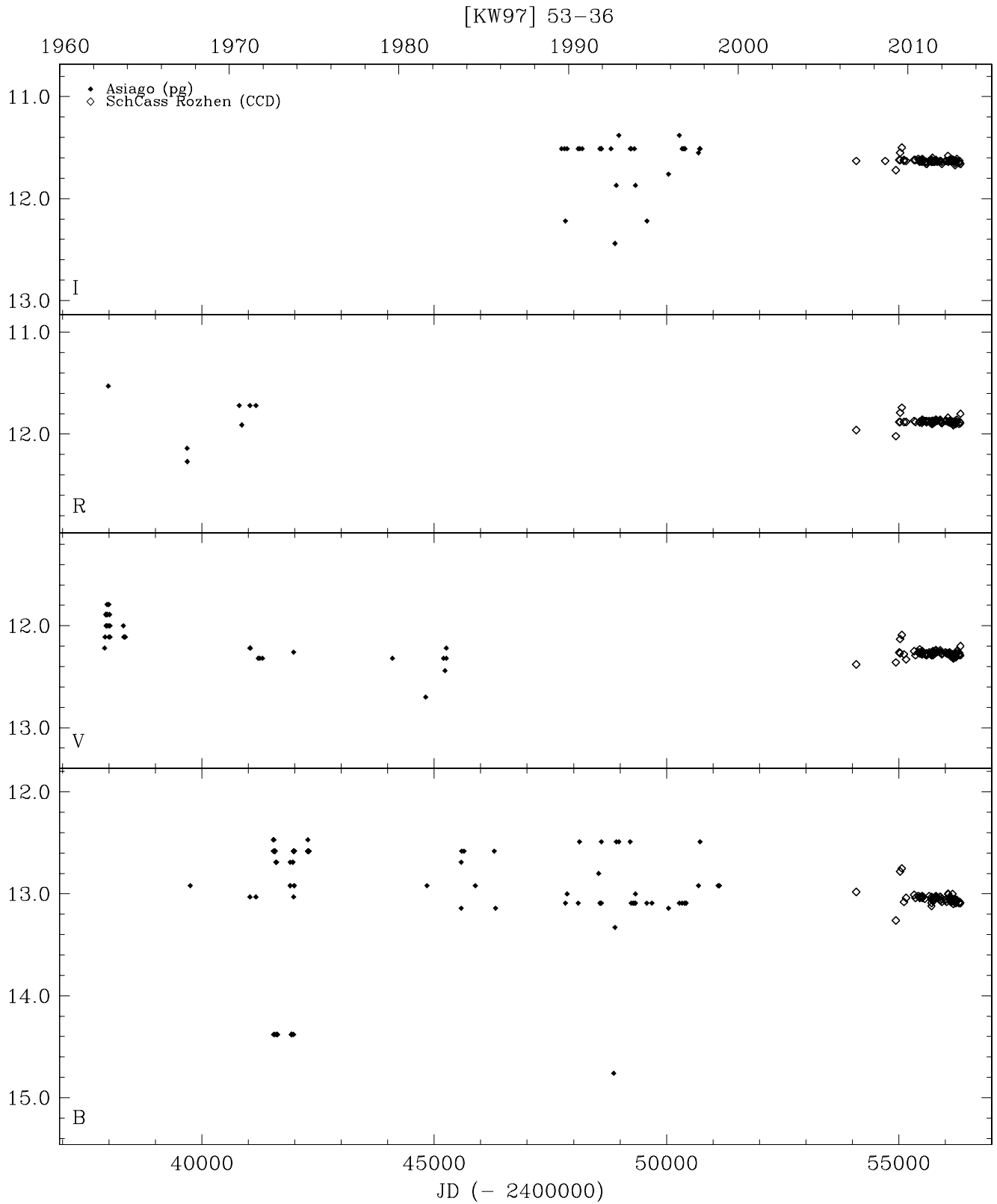


Fig. A.1. continued.

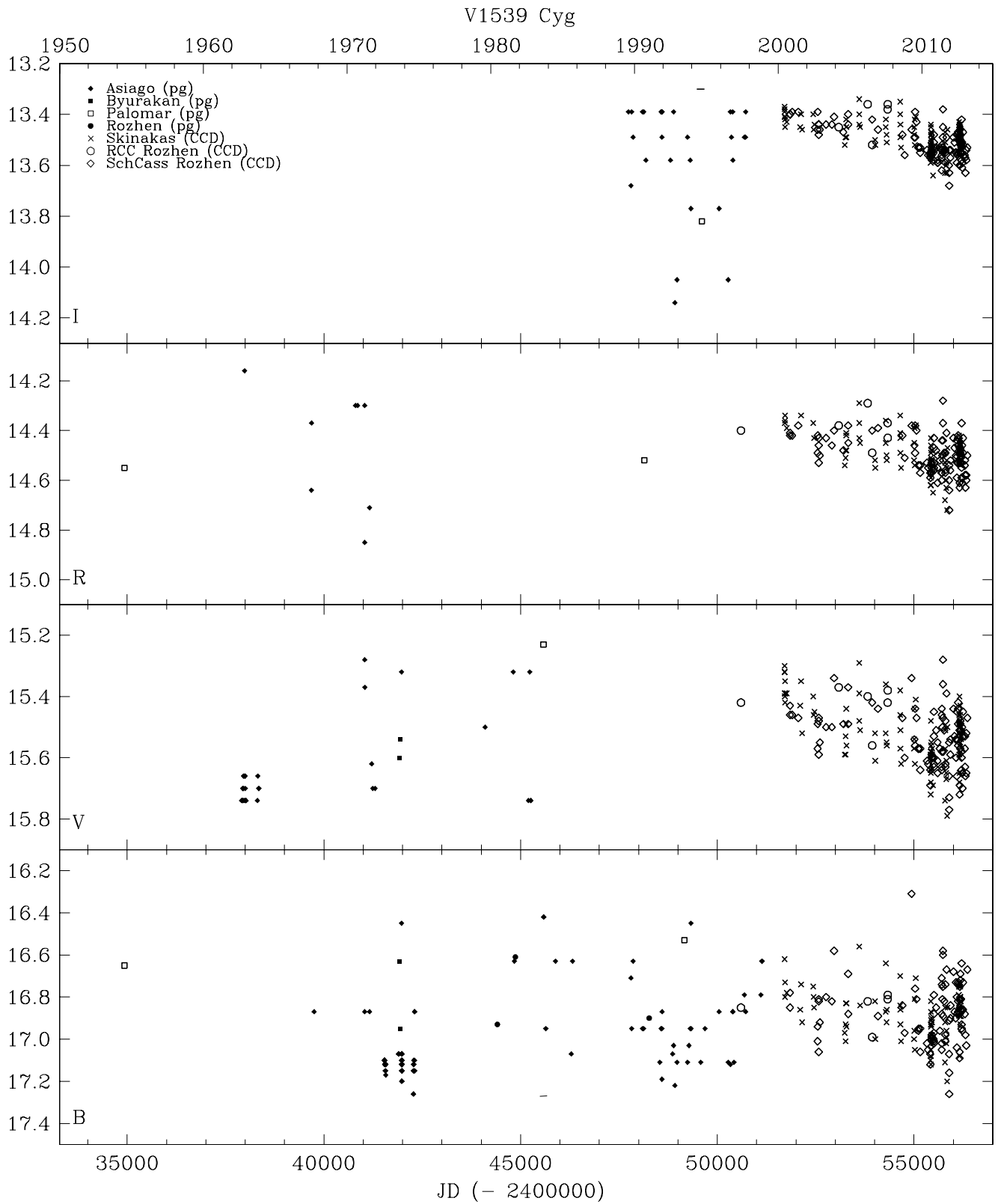


Fig. A.1. continued.

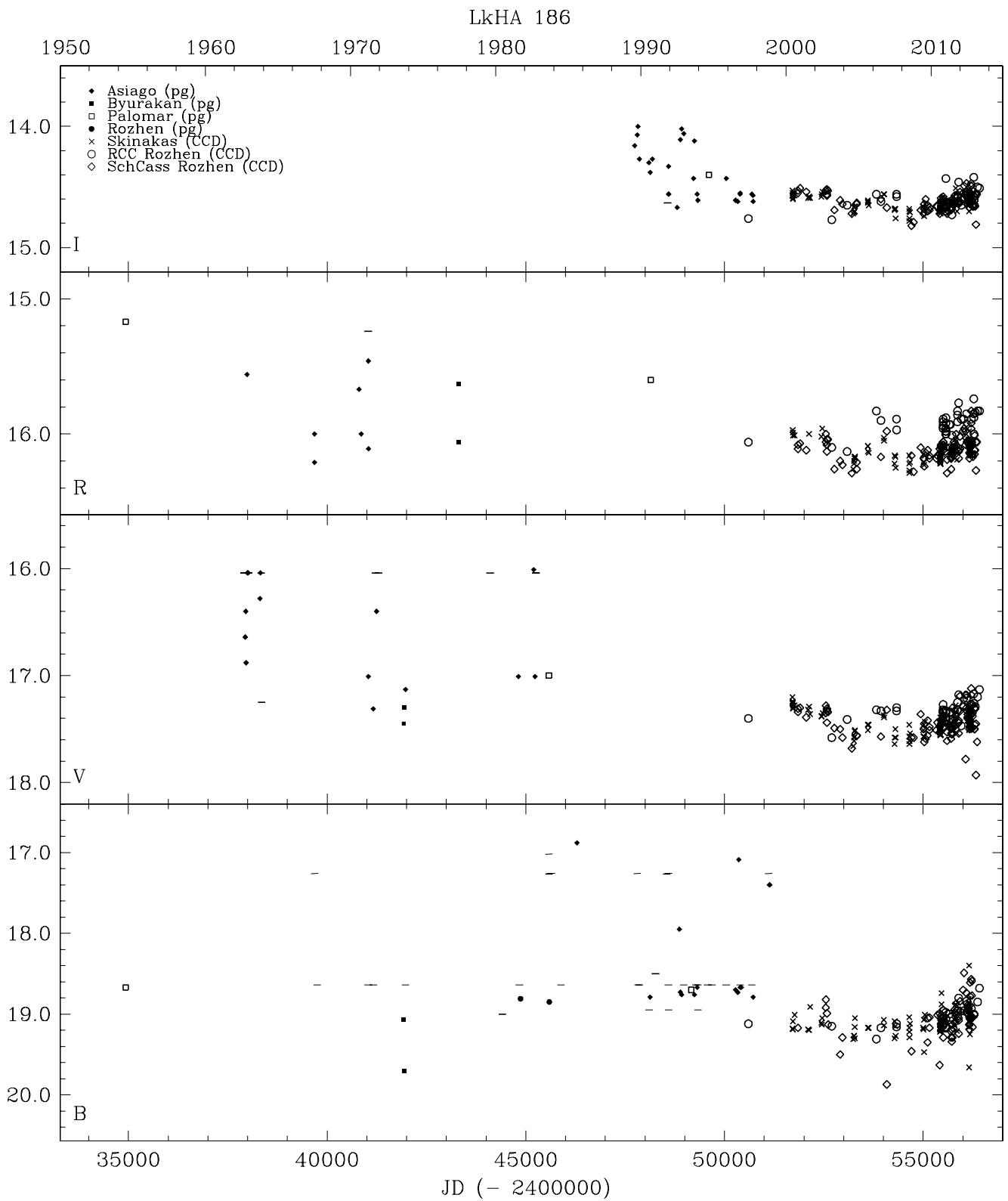


Fig. A.1. continued.

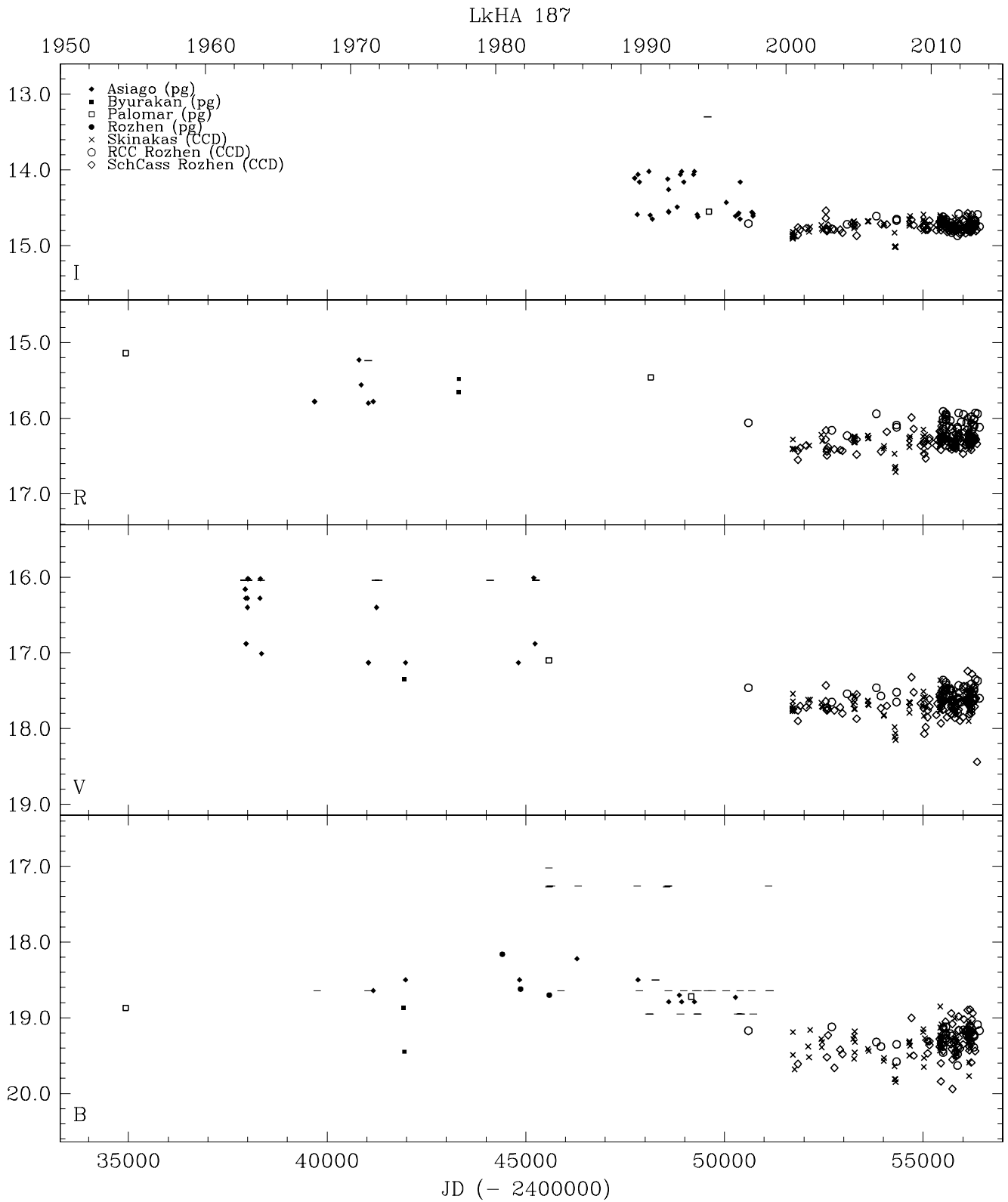


Fig. A.1. continued.

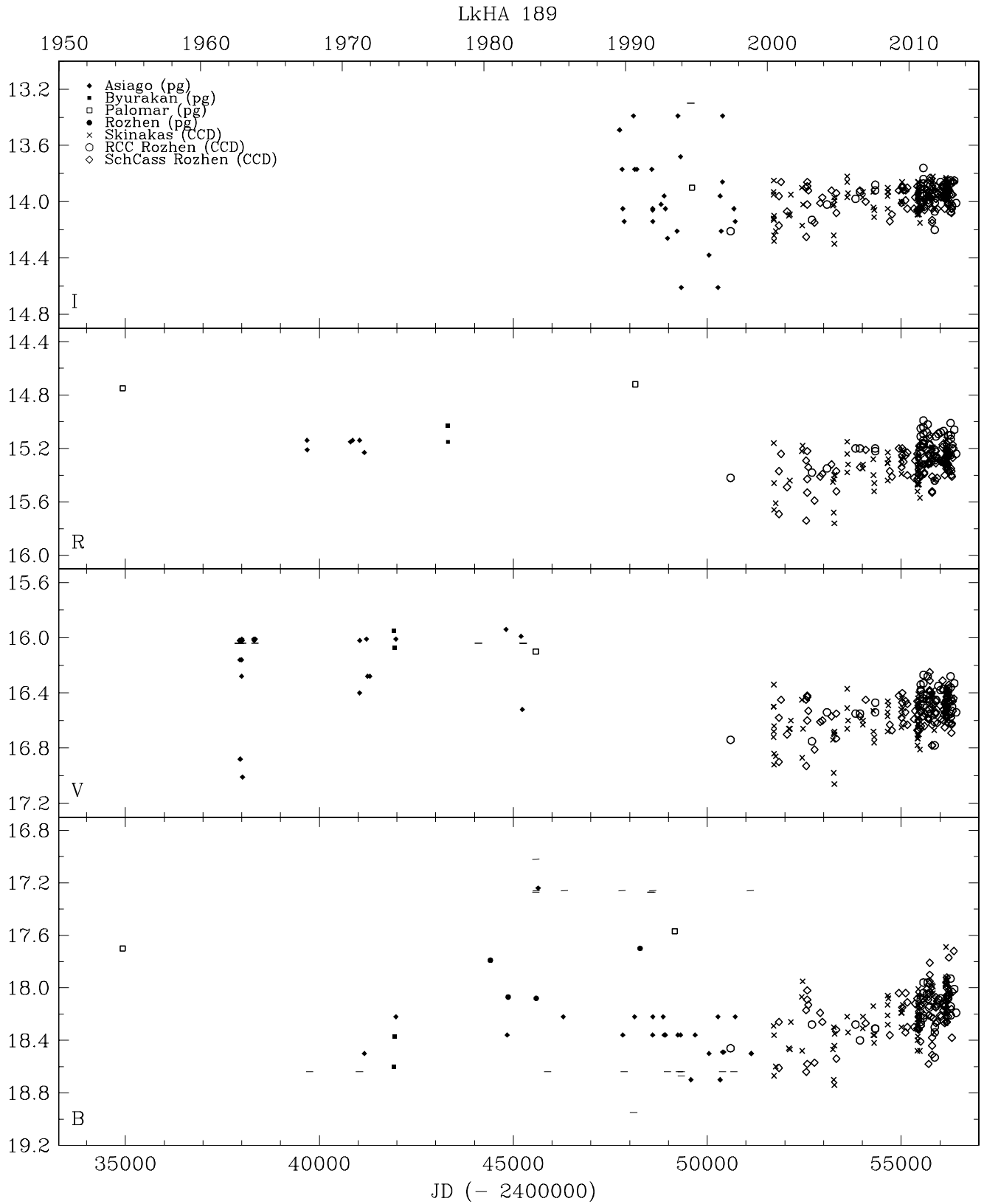


Fig. A.1. continued.

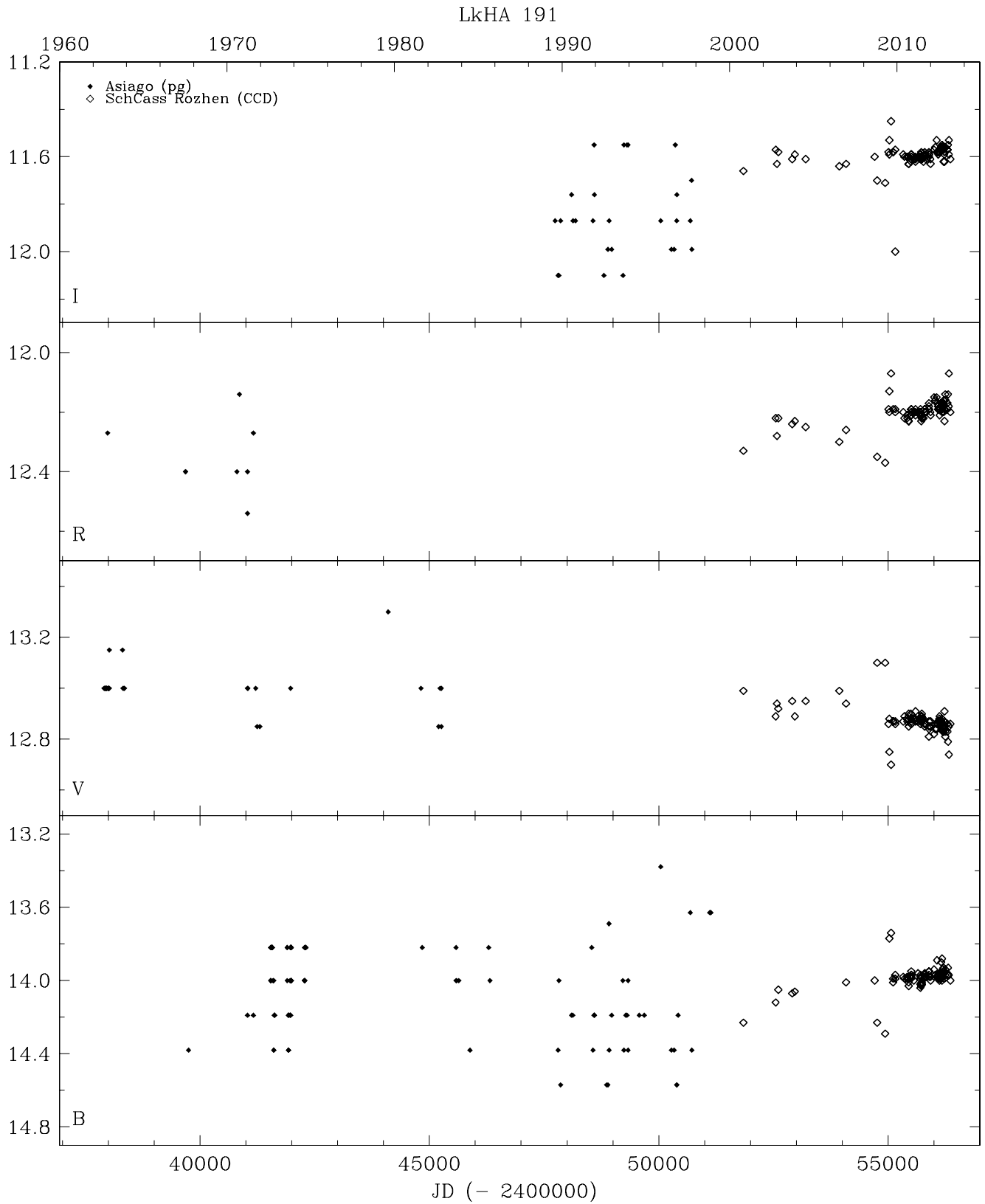


Fig. A.1. continued.

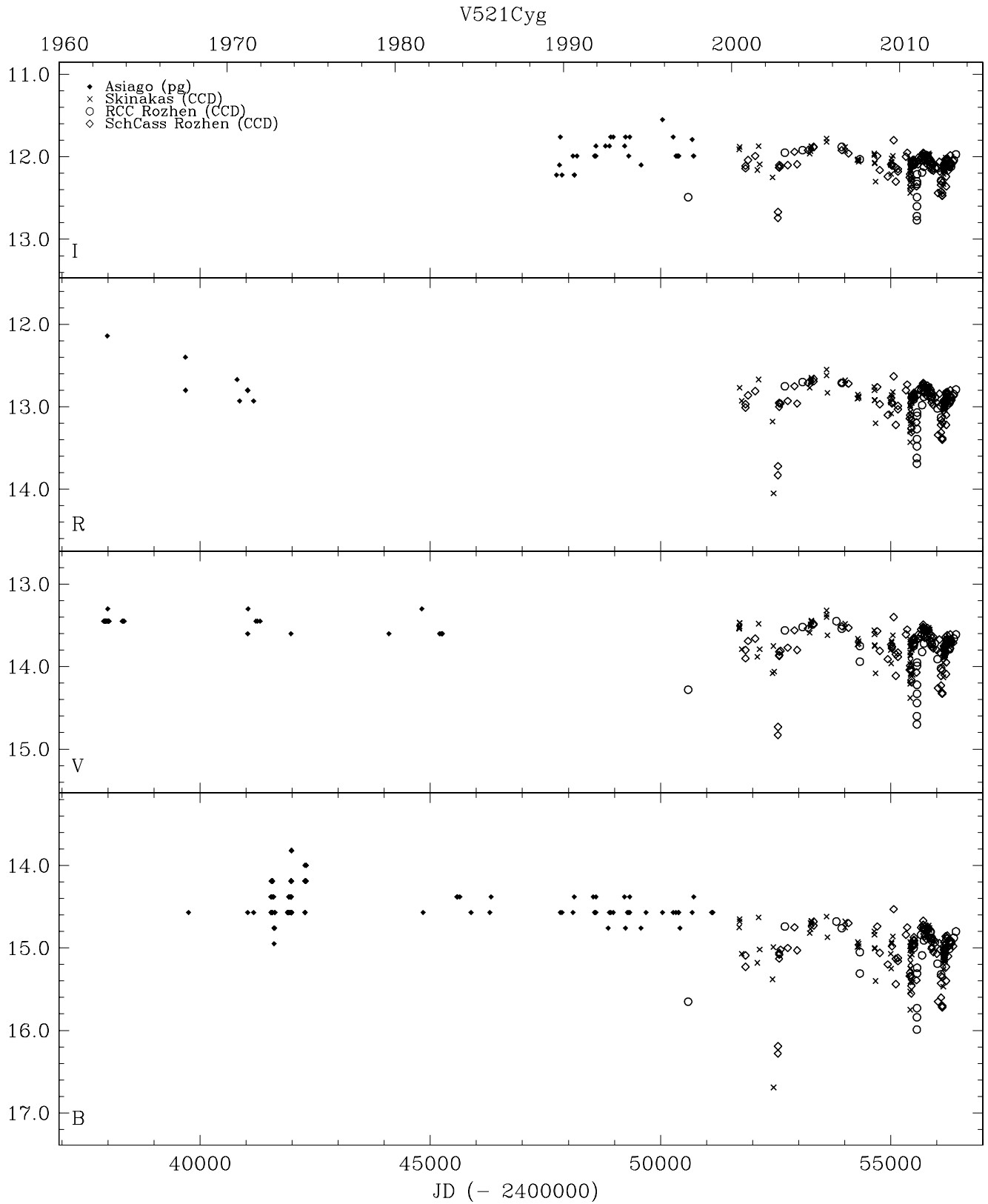


Fig. A.1. continued.

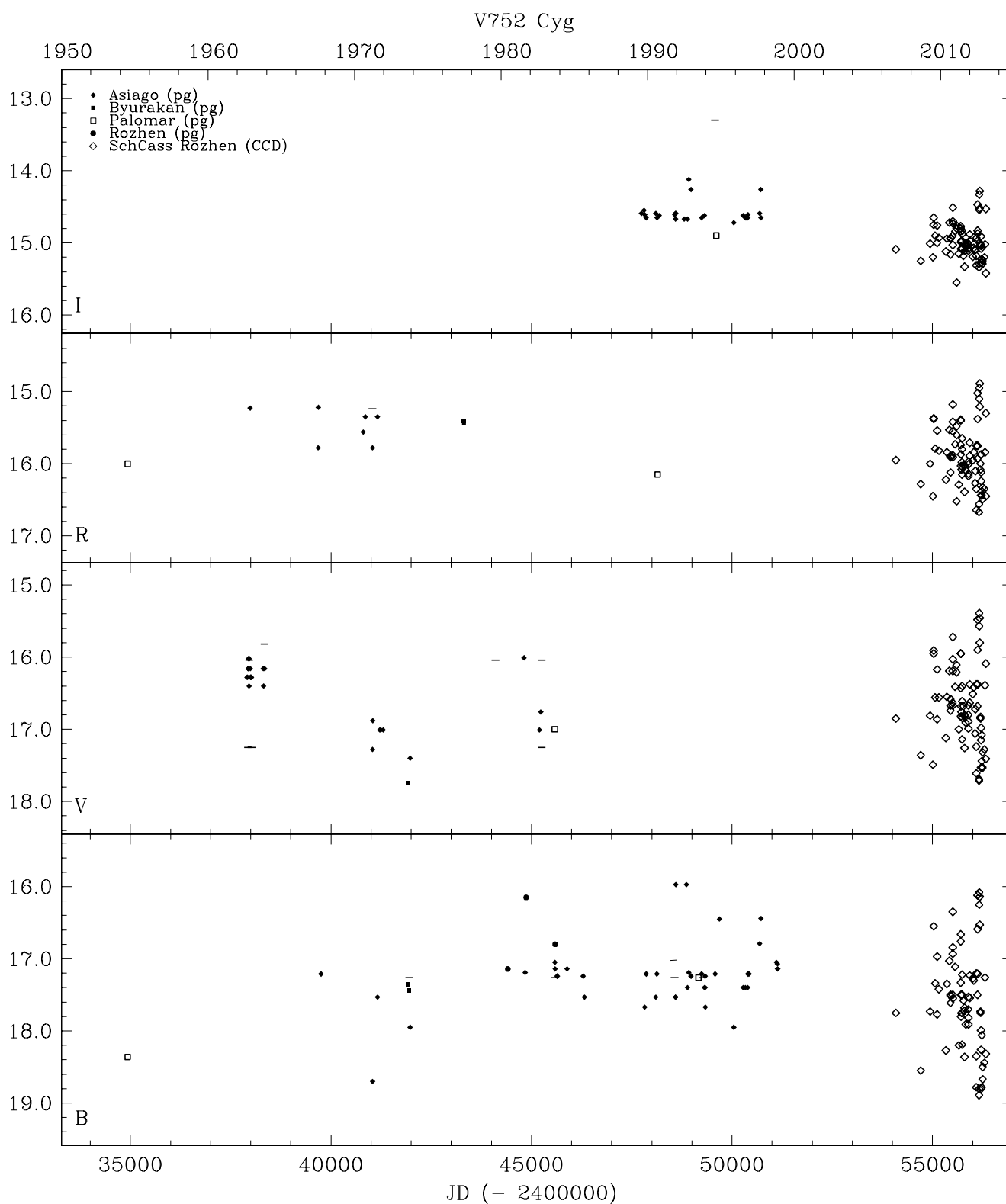


Fig. A.1. continued.

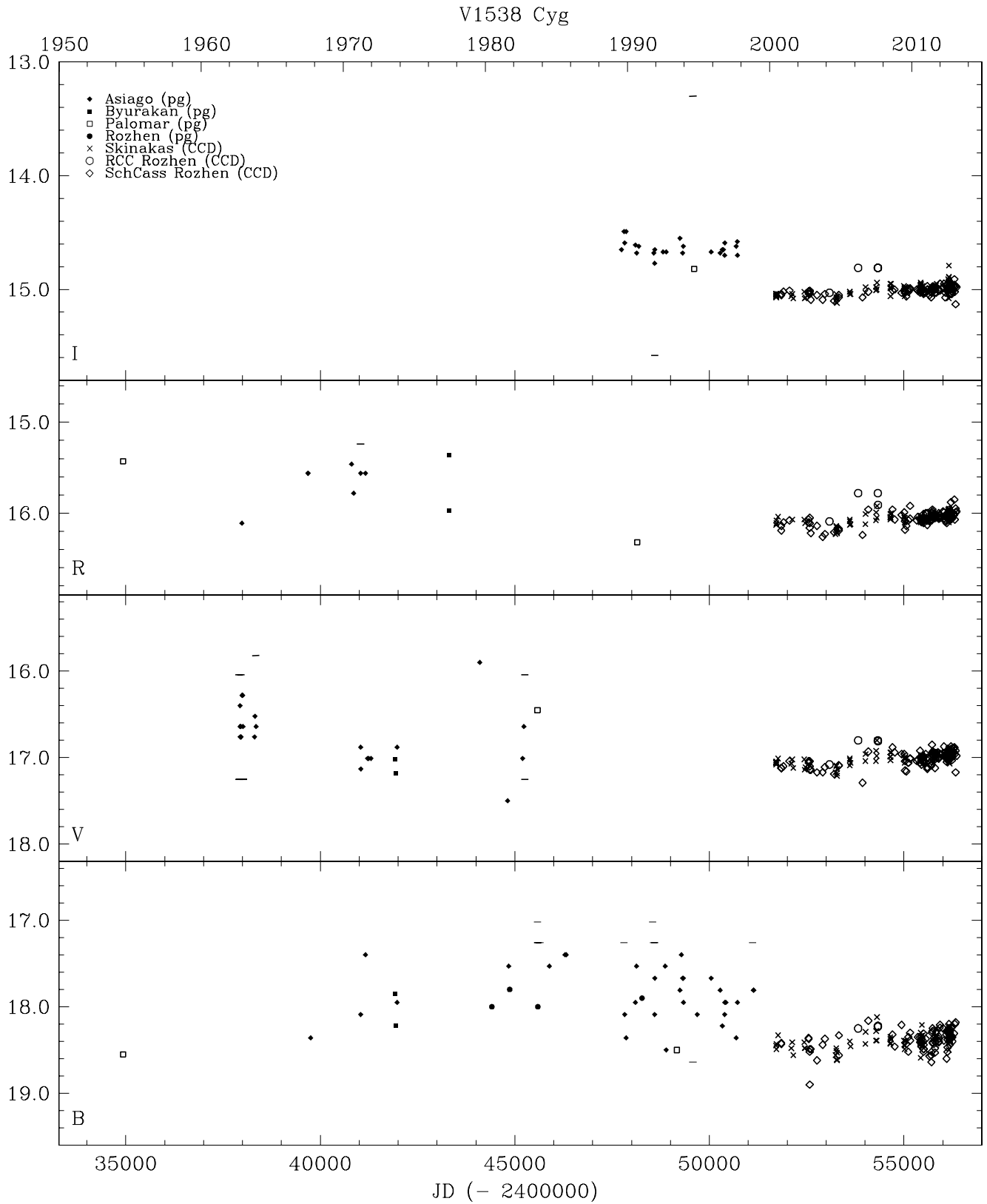


Fig. A.1. continued.

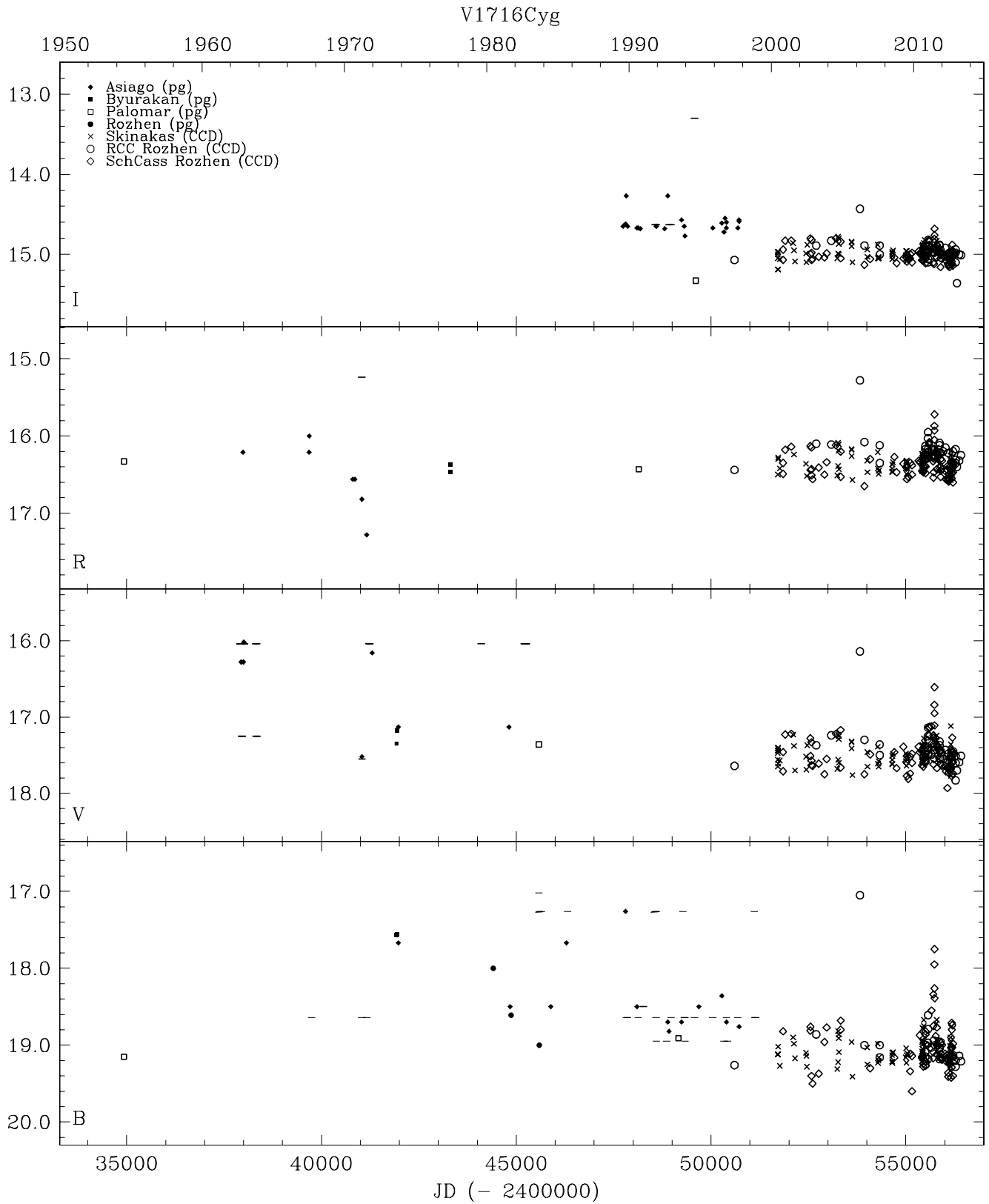


Fig. A.1. continued.

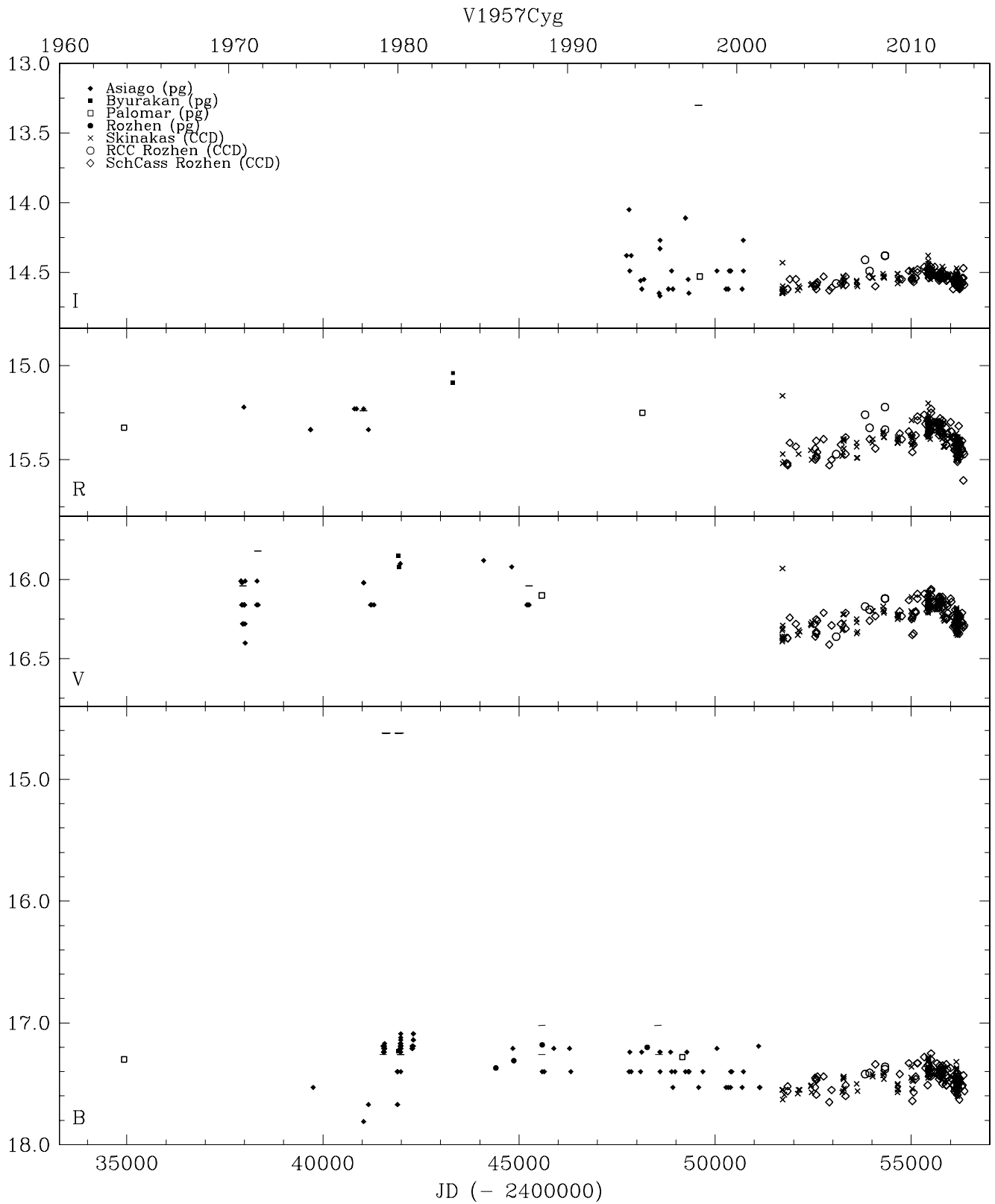


Fig. A.1. continued.

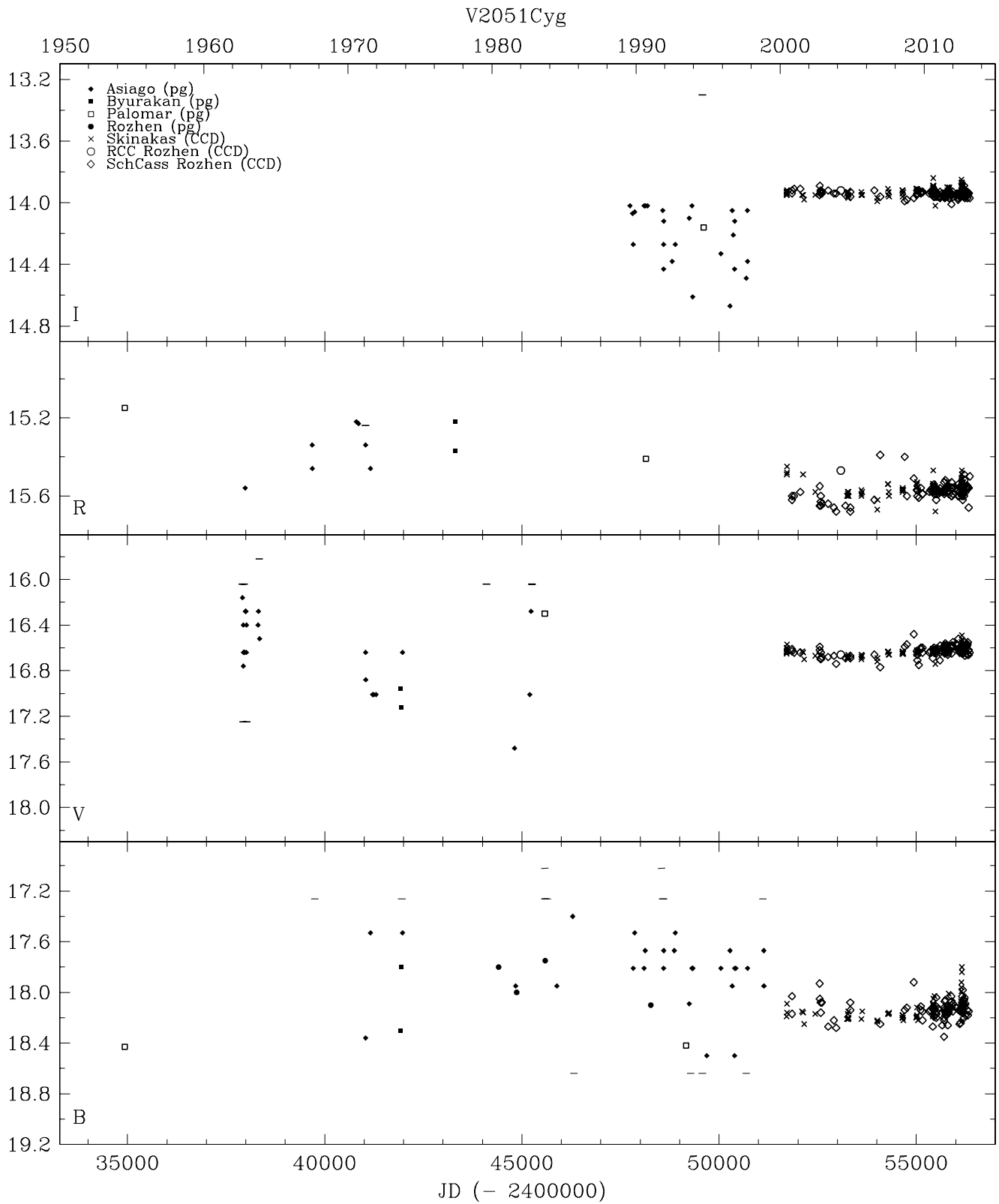


Fig. A.1. continued.